UNCLASSIFIED

SECURITY CLASSIFICATION OF THIS PAGE

REPORT DOCUMENTATION PAGE

Form Approved OMB No. 0704-0188

1a REPORT SECURITY CLASSIFICATION: UNCLASSIFIED	1b RESTRICTIVE MARKINGS: N/A
2a SECURITY CLASSIFICATION AUTHORITY: N/A	3 DISTRIBUTION/AVAILABILITY OF REPORT: APPROVED FOR PUBLIC RELEASE: DISTRIBUTION IS UNLIMITED
2b. DECLASSIFICATION/DOWNGRADING SCHEDULE: N/A	
4 PERFORMING ORGANIZATION REPORT NUMBER(S): N/A	5 MONITORING ORGANIZATION REPORT NUMBER(S): NADC-88127-60
6a. NAME OF PERFORMING ORGANIZATION: BIOMEDICAL ENGINEERING AND SCIENCE INSTITUTE; 6b. OFFICE SYMBOL (If applicable): N/A	7a. NAME OF MONITORING ORGANIZATION: NAVAL AIR DEVELOPMENT CENTER
6c. ADDRESS (City, State, and ZIP Code): DREXEL UNIVERSITY, 32nd & CHESTNUT STREETS, PHILADELPHIA, PA 19104	7b. ADDRESS (City, State, and ZIP Code): WARMINSTER, PA 18974-5000
8a. NAME OF FUNDING/SPONSORING ORGANIZATION: NAVAL AIR DEVELOPMENT CENTER; 8b OFFICE SYMBOL (If applicable): 6023	9 PROCUREMENT INSTRUMENT IDENTIFICATION NUMBER: N62269-85-C0257
8c. ADDRESS (City, State, and ZIP Code): WARMINSTER, PA 18974-5000	10 SOURCE OF FUNDING NUMBERS: PROGRAM ELEMENT NO: 62233N; PROJECT NO: MM33-I30; TASK NO: N/A; WORK UNIT ACCESSION NO.: N/A

11. TITLE (Include Security Classification)

(U) NON-INVASIVE EVALUATION OF CEPHALIC BLOOD FLOW IN THE +Gz ENVIRONMENT

12. PERSONAL AUTHOR(S)

STEPHEN DUBIN, V.M.D., Ph.D.

13a. TYPE OF REPORT	13b TIME COVERED	14. DATE OF REPORT (Year, Month, Day)	15 PAGE COUNT
FINAL TECHNICAL	FROM 7/85 TO 1/88	1988 SEPTEMBER 25	40

16 SUPPLEMENTARY NOTATION

17 COSATI CODES			18. SUBJECT TERMS (Continue on reverse if necessary and identify by block number)
FIELD	GROUP	SUB-GROUP	
06	10	10	RHEOENCEPHALOGRAPHY, +Gz STRESS, CEPHALIC BLOOD VOLUME

19 ABSTRACT (Continue on reverse if necessary and identify by block number)

Impairment of vision and consciousness under acceleration stress in the footward direction (+Gz) has been attributed to interruption of blood flow to the brain and retina. During the initial exposure to +Gz stress, the volume of blood available to neural tissues is also a significant factor because of the oxygen buffering effect of hemoglobin. The rheoencephalogram (REG) reflects changes in cephalic volume and is convenient, non-invasive and non-intrusive. Some of the drawbacks previously perceived for the REG have been ameliorated through technical innovation, while others have proven not to be of concern. Indeed the "artifact" seen with position changes and respiratory maneuvers is actually a source of useful information in the context of +Gz studies. A device has been constructed that has successfully operated under stresses as great as +14 Gz and -1.5 Gx. REG recordings have been taken from human volunteers during NAVAIRDEVCEN centrifuge rides under a variety of acceleration stress situations

20 DISTRIBUTION/AVAILABILITY OF ABSTRACT	21 ABSTRACT SECURITY CLASSIFICATION	
☒ UNCLASSIFIED/UNLIMITED ☐ SAME AS RPT ☐ DTIC USERS	UNCLASSIFIED	
22a NAME OF RESPONSIBLE INDIVIDUAL: GLORIA CHISUM, Ph. D.	22b TELEPHONE (Include Area Code): (215)441-1089	22c OFFICE SYMBOL: 6023

DD Form 1473, JUN 86 *Previous editions are obsolete.* S/N 0102-LF-014-6603

SECURITY CLASSIFICATION OF THIS PAGE

UNCLASSIFIED

and protective maneuvers and devices.

REPORT NO. NADC-88127-60
Contract No. N62269-85-C-0257

NON-INVASIVE EVALUATION OF CEPHALIC BLOOD FLOW IN THE +Gz ENVIRONMENT

by

Stephen Dubin, V. M. D. Ph.D
Biomedical Engineering and Science Institute
DREXEL UNIVERSITY
Philadelphia, PA 19104

25 SEPTEMBER 1988

FINAL REPORT
PERIOD COVERING JULY 1985 TO JANUARY 1988

Approved for Public Release; Distribution is Unlimited

Prepared for
Air Vehicle and Crew Systems Technology Department (Code 6023)
NAVAL AIR DEVELOPMENT CENTER
Warminster, Pa 18974-5000

NOTICES

REPORT NUMBERING SYSTEM - The numbering of technical project reports issued by the Naval Air Development Center is arranged for specific identification purposes. Each number consists of the Center acronym, the calendar year in which the number was assigned, the sequence number of the report within the specific calandar year, and the official 2-digit correspondence code of the Command Officer or the Functional Department responsible for the report. For example: Report No. NADC 88020-60 indicates the twentieth Center report for the year 1988 and prepared by the Air Vehicle and Crew Systems Technology Department. The numerical codes are as follows:

CODE	OFFICE OR DEPARTMENT
00	Commander, Naval Air Development Center
01	Technical Director, Naval Air Development Center
05	Computer Department
10	AntiSubmarine Warfare Systems Department
20	Tactical Air Systems Department
30	Warfare Systems Analysis Department
40	Communication Navigation Technology Department
50	Mission Avionics Technology Department
60	Air Vehicle & Crew Systems Technology Department
70	Systems & Software Technology Department
80	Engineering Support Group
90	Test & Evaluation Group

PRODUCT ENDORSEMENT - The discussion or instructions concerning commercial products herein do not constitute an endorsement by the Government nor do they convey or imply the license or right to use such products.

TABLE OF CONTENTS

LIST OF FIGURES

LIST OF TABLES

A. Acknowledgement

A major portion of this work served as material for the Ph.D. dissertation and thesis of Barry S. Shender during tenure of a research assistantship sponsored through this contract. I extend special thanks to Dr. Shender's research committee; Drs. Leon Hrebien, James Whinnery, Peter LeTarte, Thomas Moore, Donald Buerk, and Ofer Barnea for their help and encouragement.

B. Motivation of The Project

The primary motivation for this work is the detrimental effect of gravitational force in the footward direction (+Gz) upon the sensory performance of aircrew members. This is manifested as peripheral light loss (PLL) and loss of consciousness (LOC) with under certain patterns of acceleration stress. Early in the development of aerospace physiology, the effect of +Gz upon hydrostatic pressures in the circulatory system were recognized. Since then a major emphasis in dealing with the problems of PLL and LOC has been concern with maintenance of blood pressure and flow in the cerebral circulation. Our approach to this problem has begun with methods to enhance accuracy, safety and convenience in evaluation of the cephalic circulation of man and other animals in the presence of +Gz stress. As part of this study, we have begun to explore several other mechanisms; such as, cephalic blood volume, oxygen availability and local (intercellular and intracellular) transport which are involved in the genesis of PLL and LOC. As such, they are necessarily of considerable importance in our ability to anticipate the onset of PLL and LOC and to evaluate devices or maneuvers for protection.

During the past two years, we have placed major emphasis in two areas: (1) Adaptation and validation of the rheoencephalograph for use in the simulated and real aerospace environment and (2) enhancement of means for acquisition and interpretation of physiologic information as might be generated under the same circumstances.

Rheoencephalography (REG), also known as electrical impedance encephalography, is a subset of impedance plethysmography (IPG). The methods depend upon changes of volume and/or conductivity of the body segment subtended by an array of electrodes. Although the exact mechanism of the impedance variations in REG is subject to some controversy, there is no doubt as to the occurrence of pulsatile variations synchronous with the heartbeat. In the late 1960's and early 1970's, REG held high promise in clinical neurology. The method is noninvasive, convenient, and adaptable to both patient monitoring and diagnosis of cerebral vascular disorders. Some problems attributed to rheoencephalography include a relative lack of anatomic selectivity and rather major signal "artifacts" upon changes in posture (particularly in the craniocaudal axis) and respiratory efforts, such as the Valsalva maneuver.

We have chosen to use the REG for the evaluation of cephalic circulation under conditions of acceleration stress because the very same "artifact" which apparently interferes with the use of REG in clinical neurology is of critical interest in G studies; namely, the bulk movement of blood between the head and the rest of the body with postural changes and respiratory maneuvers. Also, we are interested in studying total cephalic circulation not just the intracranial component.

By way of comparison with other methods of investigating cephalic circulation in the +Gz environment, REG offers several important advantages. It is virtually innocuous in terms of danger to the subject, discomfort, inconvenience, and constraints upon the performance of mission-oriented tasks. It is objective, in that it does not depend upon a response or participation of the subject. The readings are continuous and seem to reflect circulatory changes instantaneously. The equipment is relatively simple, inexpensive and potentially "G-tolerant." REG is quite suitable to evaluation in experimental animals. A tractable but non-trivial task has been to assess the validity of REG as a method for evaluating cephalic circulation in the +Gz environment and to provide suitable instrumentation for the same purpose.

In view of the qualities listed above, rheoencephalography poses excellent promise for monitoring the cephalic circulation in +Gz environmental stress. The limitations of REG as a clinical tool in the diagnosis of specific vascular lesions are much less important in the aerospace monitoring setting.

C. Goals

As stated in our original proposal, the project goals fall into three categories. (1). Equipment Development: Development and testing of a REG instrument which will reveal both the pulsatile component of cephalic blood flow and the bulk shifts of blood between the head and trunk resulting from G forces. The instrument must be physically robust enough to operate on the human centrifuge and have maximal safety and convenience for the subject. (2). Animal Experiments: Animal experiments will be used for those investigations where there must be prolonged experimentation and when it is desired to compare the REG with invasive methods which are undesirable for human subjects. (3). Human Studies: Initial human evaluations are devoted to proper conformation and location of electrodes and to verification of safety of the instrument. In coordination with the centrifuge schedule at NADC, REG was to be recorded on human subjects during centrifuge rides under a variety of acceleration stress situations and protective manuveurs.

D. Implementation and Results

(1). Equipment Development:

The basic design of the rheoencephalograph is, conceptually, very simple. The body segment to be examined is connected to a resistance bridge. The excitation source of the bridge is generally sinusoidal in the frequency range of 15 to 150 kHz. Currents in this frequency range will not effectively stimulate the heart or skeletal muscle. The output of the bridge is amplified and demodulated. A major challenge in recording the REG is the composite nature of the impedance changes that are recorded. The resting baseline impedance is determined by the composition (blood, bone, etc) of the body part being examined, its geometry, and the electrode interface. Bulk shifts of blood, such as result from venous occlusion of a limb, the Valsalva maneuver or G forces cause changes in the range of 1-2% of the total baseline value. Resistance changes resulting from arterial pulsations are three orders of magnitude smaller than the baseline resistance. With previous circuits and display devices, acquisition of the pulsatile component resulted in loss of much information about the bulk blood shifts.

Much of our initial work has been devoted to application of more recent improvements in electronic instrumentation, including digital methods, to the acquisition of the REG. In our REG design, real time signal processing has been a priority. Among the technical problems we have addressed are separation of baseline impedance (Zb) from change in impedance due to pulsatile variation in blood volume (ΔZ), amplification of ΔZ and Zb, noise reduction, shock hazard reduction, electrode configuration and G "hardiness."

The difference in frequency content between Zb and ΔZ is on the order of a few hertz, so one cannot simply low pass filter to separate the two. We chose an analog method employing an integrator with a very long time constant (0.74 sec) to average the variation in the signal and extract Zb and an analog summing amplifier using this signal and the composite (Zb + ΔZ) to obtain ΔZ. This also serves to reduce the "baseline drift" problem. The magnitude of ΔZ is on the order of 10 to 40 mV peak-to-peak and is imposed on a dc offset that can vary from subject to subject. In order to obtain sufficient signal strength for processing, ΔZ must be amplified approximately 100 times. Since the fundamental frequency of ΔZ is 1 to 3 Hz, removal of the offset prior to amplification is done with a procedure very similar to the one above.

According to Nyboer (Electrical Impedance Plethysmography. Springfield, Illinois Charles C. Thomas, 1970), when stimulated by a frequency between 100-1000 kHz, a biological segment becomes a pure resistance and the reactive factors approach zero. We chose to use a sinusoidal carrier signal at 100 kHz so that volumetric changes will be directly related to conductance. Since 100 kHz is a radio frequency, the power lines and all IC components are capacitively protected and the 100 kHz oscillator is mechanically shielded. Prior to AM demodulation, the REG signal is processed through a narrow (approximately 2 Hz) analog band pass filter centered about the carrier frequency. Noise reduction is further improved prior to amplification of ΔZ by using a Reticon™ 7 pole, 6 zero elliptic low-pass filter. This filter has a precipitous cuttoff at 12 Hz, minimizing motion artifacts. Shock hazard to the subject is reduced by using battery power and components are selected for low power consumption and low noise. To make the instrument easier to use and to simplify the circuitry, we chose to use a bipolar electrode arrangement with an additional ground

reference electrode. Exact placement of two electrodes on the head, when used in a bridge detection circuit, is not as critical as in the typical tetrapolar configuration.

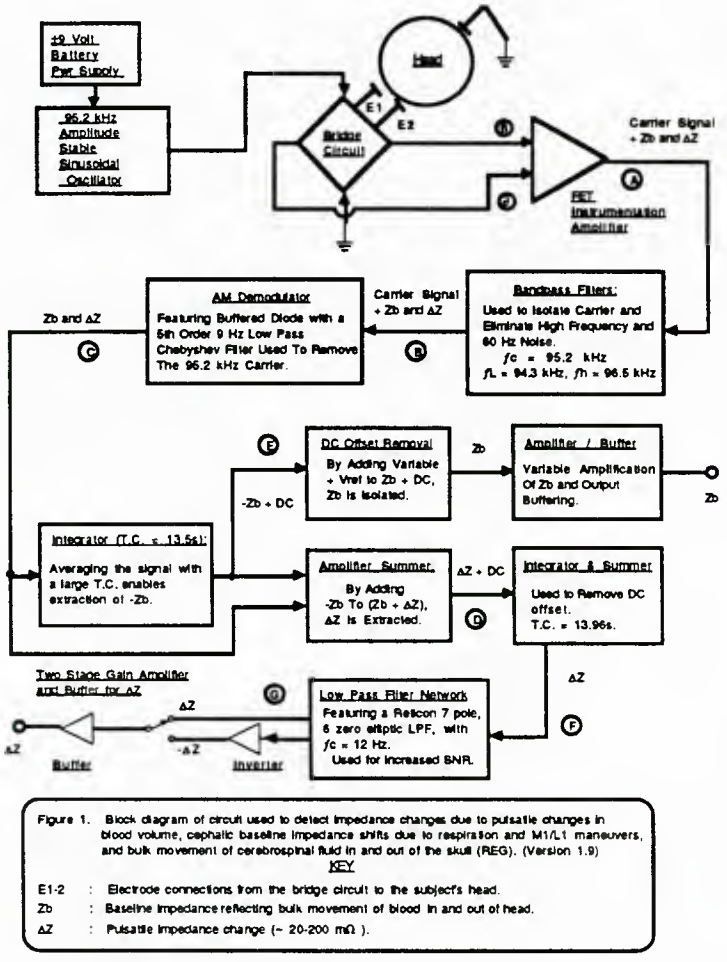

Figure 1. Block diagram of circuit used to detect impedance changes due to pulsatile changes in blood volume, cephalic baseline impedance shifts due to respiration and M1/L1 maneuvers, and bulk movement of cerebrospinal fluid in and out of the skull (REG). (Version 1.9)

KEY

E1-2 : Electrode connections from the bridge circuit to the subject's head.

Zb : Baseline impedance reflecting bulk movement of blood in and out of head.

ΔZ : Pulsatile impedance change (~ 20-200 mΩ).

A block diagram of the "NADC REG" is given in Figure 1. The principle underlying the operation of the device is as follows. The head comprises the unknown resistance of a modified Wheatstone bridge, which is excited by a 95.2 kHz sinusoidal voltage. The head can be considered as a series combination of impedances; a low frequency component coincident with heart rate, a dc value comprising the impedance of the head, skin, and neural tissues, and a baseline impedance which is modulated by the low frequency impedance. The bridge output therefore consists of an amplitude modulated high frequency carrier riding on a dc offset. This AM signal is passed to a high input impedance instrumentation amplifier. This stage does not load the bridge, i.e. draw current, and eliminates unwanted noise signals common to the differential bridge output. The AM signal is processed by a narrow bandpass filter tuned to attenuate all but the carrier frequency. The signal is then demodulated via a classic diode-low-pass filter combination to remove the carrier. The baseline impedance is separated from the low frequency impedance via a slow integrator-subtraction circuit. Both waveforms are then amplified and buffered for transfer to display and recording devices.

In designing this device, among the major considerations were portability, safety (isolation), sensitivity, low noise and real-time processing of the impedance signals. The REG is battery operated and includes the use of low-power IC chips in order to avoid most patient isolation problems, particularly those associated with line frequency electric shock. All electrical connections to and from the head and the output signals are all buffered with operational amplifiers. Battery power allows the device to be portable and allows more flexibility when it comes to installing it in the centrifuge gondola at NADC for acceleration studies. A problem that occurs with these devices is that when one obtains a differential signal from the head of the subject, the signal can be eliminated by the patient touching a metal object. In order to overcome this phenomenon, the earlier versions of the device included placement of an additional ground electrode on the subject in an attempt to create a common reference level between the device and the centrifuge gondola.

The newest version of the device, to be tested in 1989 at NADC, employs the use of a high frequency 1:1 matching transformer (3 MHz) to isolate the patient and a dual battery power supply. A ±9 volt power source consisting of two 9 volt batteries, will energize the front end. The front end (i.e. the oscillator) will then have a totally separate ground from the subject and any potential ground loops will be effectively eliminated. The currently used ±9 volt supply (12 "C" batteries) will power the back end (i.e. the processing circuitry). Figure 2 shows the details of the battery power supplies. The third electrode, the ground, will then be no longer necessary. Patient isolation will be assured and electrode application will be further simplified.

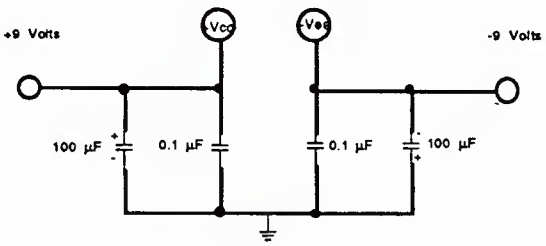

Figure 2. REG Battery Power Supply.
Back end includes 12 "C" Alkaline Batteries
Front end includes 2 9 volt Alkaline Batteries

The REG splits the impedance signal obtained from the head into two components in real time: 1) impedance changes referable to the pulsatile variation in blood volume (ΔZ), and 2) the "baseline" impedance which is an indication of the bulk movement of blood between the head and the rest of the body (Zb). Unstressed ΔZ ranges from approximately 470 to 530 mΩ. ΔZ and Zb are primarily resistive quantities at 100 kHz as evidenced by the low phase shift measured between the oscillator output and the instrumentation amplifier output . When the skin-electrode interface is properly prepared, i.e. skin cleansed with alcohol, good adhesion of the surface electrodes, etc., the phase shift is approximately - 3.5°. This indicates a capacitive shift in the signal caused by the head. If skin preparation is inadequate, the phase shift can be as high as -27°, due to skin capacitive effects.

Since the aim of this REG is to obtain a relative measure of the overall state of the cerebral blood circulation and not to diagnose deep cerebral incidents, a bipolar (two electrode) design for the excitation/receiving electrodes was chosen. A bipolar arrangement is highly sensitive and can detect very low level changes better than a tetrapolar system. The sensitivity of the bridge transducer is 0.7 mV/Ω. The output of the device is linear beyond the expected range of ΔZ, i.e. 0 - 50 Ω, assuming a basal resistance of the segment of 1 kΩ. This was derived by plotting a regression line for sensitivity (S = d Vout/d R) versus change in resistance.

The equation was

$$S = -7.07 \times 10^{-4} + 3.65 \times 10^{-6}\, dR \qquad \text{eq. 1}$$

where the coefficient of determination, R^2, was 0.861. With amplification, the ΔZ output voltage ranges from 350 to 750 mV/Ω. This arrangement also has the added benefit of simpler circuit design and ease of experimental setup. With a bipolar configuration, the electrode placement on the subjects is simplified as compared to the tetrapolar arrangement (which uses a constant current source activating two excitation, with two receiving electrodes between them).

In order to promote safety and record a signal that essentially contains all real (no reactive) components, a sinusoidal excitation frequency of 95.2 kHz, ±1.4 volts peak-to-peak, produced by an amplitude stable sinusoidal oscillator (see Figure3), is used to energize a resistance bridge.

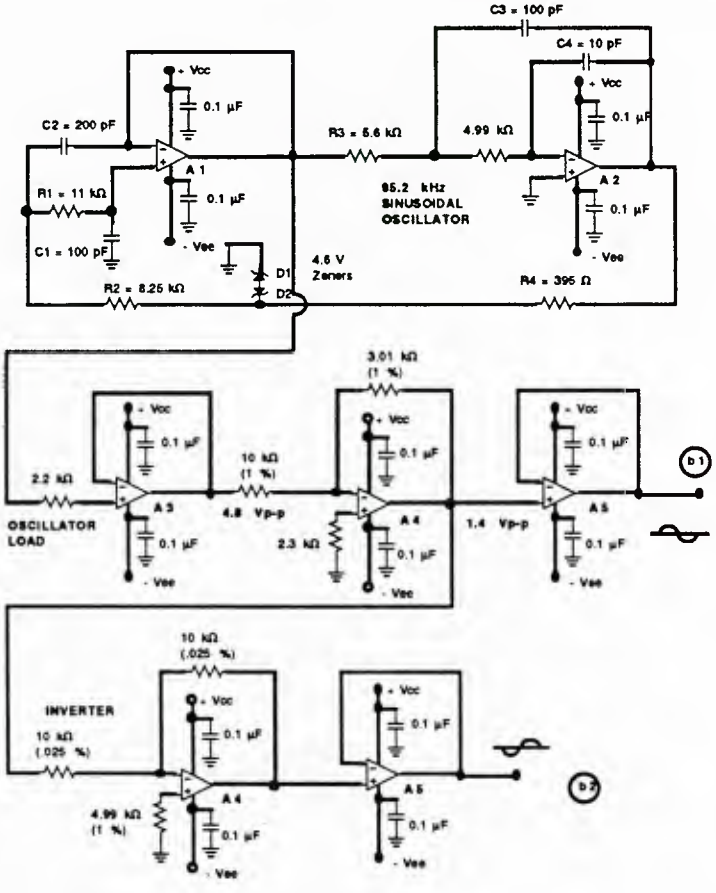

Figure 3 95.2 kHz Amplitude Stable Sinusoidal Oscillator, Gain Reduction Stage, and Inverter for ± Signal Excitation To Detection Bridge

KEY

A1,2 : LF 351 Oscillator.
A3 : TL071 Load/Buffer Stage.
A4 : 1/2 TL072 Gain Reduction/Buffer Stage.
A5 : 1/2 TL072 Signal Inversion/Buffer Stage.

In Figure 3, operational amplifier A1 is connected as a two-pole low pass active filter (LPF) and A2 is configured as an integrator. This combination of op amps oscillates when the loop gain is

high enough at the frequency in which the phase lag of the amplifiers is 180°. The amplitude is stabilized via zener diodes D1 and D2. The distortion introduced by these diodes is reduced by the LPF. Since D1 and D2 have essentially equal breakdown voltages, the resulting symmetrical clipping virtually eliminates the even order harmonics. The third harmonic is approximately 40 dB down at the output of A1, leading to a total harmonic distortion of about one percent. Oscillation frequency and threshold are set by R1, R2, R3, C1, C2, C3, and C4. R4 is set much smaller than R2 so that the effective resistance at R2 does not drop when the zener diodes conduct.

A3 acts as an oscillator load and buffer stage. Half of A4 serves to reduce the gain (Av = -3.01 kΩ / 10 kΩ = 0.33) and current consumption. The other half of A4 employs high precision (0.025%) resistors to shift the sine wave 180° for a ± excitation source for the bridge. The two output waveforms from A4 are passed through buffer stages (A5) prior to connection to the transformer (see Figure3, points b1 and b2).

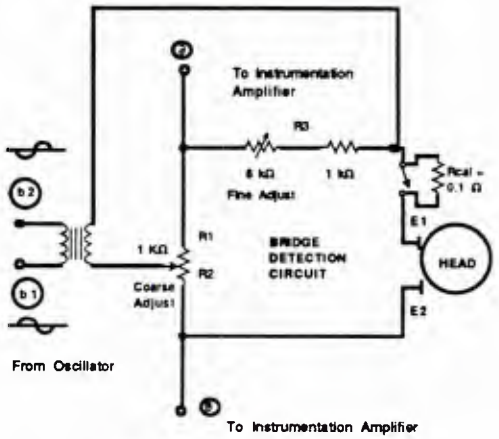

Figure 4. Newest version of Bridge Detection Circuit. Note bridge is excited by ± sinsuoidal voltage. There is no grounding electrode attached to the head. 1:1 matching transformer added to isolate excitation voltage from subject.

Rcal — Calibration Switch - Normally closed, when opened adds 0.1 Ω to head.

E1, E2 — Electrodes affixed to subject.

Details of the improved bridge detection circuit (Figure 4) design are as follows. The major changes include a ± excitation voltage as opposed to a single ended approach. This effectively eliminates the previous need for an inversion switch prior to ΔZ output. The bridge also receives slightly more current than previously. The potential value of the variable resistance arm of the bridge has been increased. This will enable setting the bridge to correct operating levels with wider swings in the basal resistance of the head (primarily due to the skull and electrode interface). The elimination of the third electrode should increase detectable signal power.

Due to the small size of the signal in relation to the relatively large dc offset that occurs at this point in the circuit, the bridge is operated "off-null" and balancing the bridge entails changing its variable resistors (large swing and fine adjustment) until a maximum amplitude signal is obtained. Included in the bridge is a 0.1 Ω calibration resistor used to both correlate a fixed ohmic change to a voltage excursion and to provide a quick check that the device is operating properly. Since the value of the calibration resistor is so low, it is connected to a low resistance (10 mΩ) miniature SPDT toggle switch (ALCOSWITCH #MST-105E).

To describe the bridge output voltage, the resistors are described as follows. The "coarse ad-

just," a 1 kΩ 10-turn precision wirewound potentiometer (Spectrol model #534), is used to correct the output voltage based on the unknown resistance of the head. The excitation sinusoid is applied to the wipe of the potentiometer and its two portions can be described as 1 kΩ - X Ω (R1) and X Ω (R2). The unknown resistance is expressed as a series combination R3 + ΔR3, where R3 is the dc resistance and ΔR3 is the small change due to changes in blood volume, of both pulsatile and bulk movement origins. R4 is the series combination of the "fine adjust" potentiometer and a fixed 1 kΩ resistor. The latter is used to help keep the bridge off null. Typical base dc resistance of an entire mammalian head ranges from about 80 - 1000 Ω. Assuming proper skin preparation, this arrangement requires very little bridge adjustment among individual subjects; a very useful feature when one considers the high cost of delays in human centrifuge experimentation. Classical analysis of the bridge leads to the following equation for output voltage, Vout, which will vary based on ΔR3, based on the above fixed resistances which form two potentiometric dividers across the excitation voltage, Vin:

$$V_{out} = \frac{R_{in} V_{in}}{R_1 + R_4} - \frac{R_2 V_{in}}{R_2 + (R_3 + \Delta R_3)} \qquad \text{eq. 2}$$

or

$$V_{out} = \frac{[R_1/R_4 - R_2/(R_3 + \Delta R_3)]\, V_{in}}{(1 + R_1/R_4)(1 + R_2/(R_3 + \Delta R_3))} \qquad \text{eq. 3}$$

Once the head is excited, an amplitude modulated composite signal, Zt, (ΔZ+ Zb + carrier) is passed into a FET instrumentation amplifier (IA) to detect a differential signal off of the head and to ohmically isolate the subject (see Figure 5). Output offset votage is removed from the IA from a voltage divider between pins 1 and 5 of op amp A7. The overall voltage gain, Av, of the IA is

$$Av = [(2\ Ra/Rc) + 1][R8/R6] \qquad \text{eq. 4}$$

if Ra = Rb, R6 = R7, and R8 = R9 + R10. R10 is used to maximize common mode rejection. Ra, Rb, R6 and R7 are 1% precision resistors to ensure that the equalities hold.. Rc sets the gain. The capacitors used in A8 serve to minimize the frequency response of the IA above 100 kHz. The overall gain is set at 42. This was a compromise between reasonable gain and the high input impedance of the FET op amps. The common mode rejection ratio is 60 dB at 100 kHz.
Zt is then placed through a cascade of two active filters comprising a narrow bandpass filter section (BPF), centered about the carrier frequency, which reduces high and 60 Hz frequency noise (see Figure 6). The first section is a biquad BPF, which is characterized by a constant absolute bandwidth . The gain of the filter, K, is variable as determined by R1 (series combination of a 20 kΩ potentiometer and a 3.9 kΩ fixed resistor) and R2. The Q of the filter is set by R2 and the center frequency, ω_0, is set by R3 and C1. The transfer function for this BPF is given by:

$$H(s) = \frac{K\,\omega_0 s/Q}{s^2 + s\omega_0/Q + \omega_0^2} \qquad \text{eq. 5}$$

where Q = 20, 1.4 ≤ K ≤ 8.6, ω_0 = 613.2 x 103 rad/s (97.6 kHz), Vout = output voltage, Vin = input voltage, and bandwidth = 7 kHz. To choose the values of R1 - R4 and C1, these factors were first normalized: ω_0 = 1 rad/s, C1 = 1F, and R4 = 1Ω. Then R1 = Q/K, R2 = Q, and R3 = 1Ω. To denor-

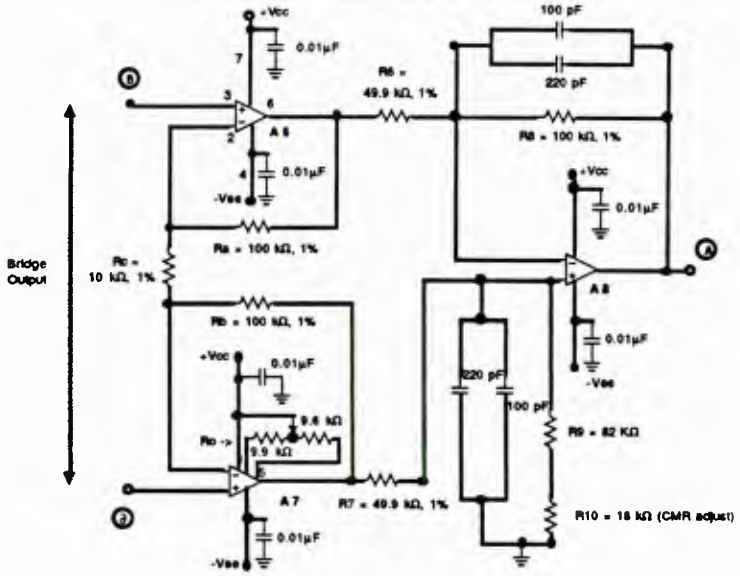

Figure 5. Instrumentation Amplifier - Low Pass Filtered To Eliminate High Frequency Noise.

KEY

A6-A8 : LF356N.
Rc sets the gain for the front end (Gain = 21).
R6 sets the gain for the back end (Gain = 2). Overall Gain = 42.
at Ro is a resistor pair that provides DC offset control.
Input voltage is on the order of 20 mV.

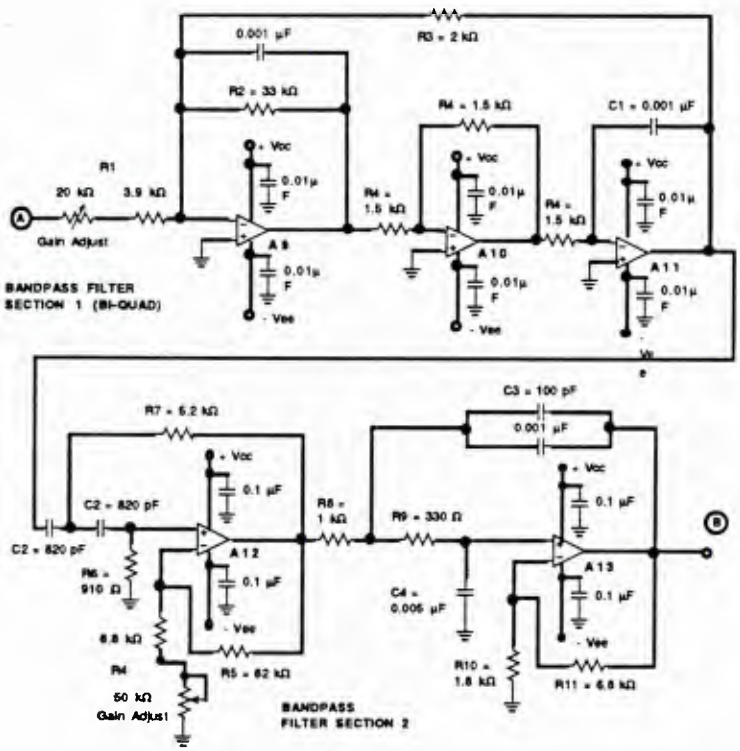

Figure 6. Bandpass Filters - Eliminates Both High and Low Frequency Noise Interference While Retaining AM Modulated Carrier.

KEY

A9 - A13 : LM318N.
f_c (Center Frequency) = 95.2 kHz Sinusoidal.
f_L (Lower 3 dB Frequency) = 94.3 kHz Sinusoidal.
f_h (Higher 3 dB Frequency) = 96.5 kHz Sinusoidal.

malize these values, the frequency normalizing factor, μ, and the impedance scaling factor, ISF, were calculated as follows:

$$\begin{aligned}\mu &= \omega_o/\omega_n \qquad \text{eq. 6}\\ &= 2\pi f_o/1 \text{ rad/s}\\ &= 2\pi(100000)/ 1 \text{ rad/s}\\ &= 200000\pi ,\end{aligned}$$

where the subscript n refers to the nomalized value and

$$\begin{aligned}\text{ISF} &= f_o/20\pi \qquad \text{eq. 7}\\ &= 100000/20\pi\\ &= 1591.55.\end{aligned}$$

Then the capacitances and resistances were calculated as

$$C = C_n/\mu\text{ISF} \qquad \text{eq. 8}$$

$$R = \text{ISF}(R_n). \qquad \text{eq. 9}$$

$$H(s) = \frac{K s^2}{a_0 + a_1 s + s^2} \qquad \text{eq. 10}$$

To improve on this stage, a second active BPF was added which consists of a cascade of a second order Chebyshev voltage controlled voltage source (VCVS) high pass filter (HPF) and a second order VCVS LPF. The transfer function of the HPF is given by:
where the variable gain, K, is set by R5/R4 + 1 and ranges from 2 to 10. R4 is the series combination of a 50 kΩ potentiometer and a fixed 6.8 kΩ fixed resistor. The Chebyshev coefficients, for a 0.5 dB ripple width (ripple factor = 0.349), are a_0 = 0.66 and a_1 = 0.94. The cutoff frequency is set at 90 kHz. C2 was normalized to 1F. Normalized conductances were found by using equations 11 and 12.

$$G_7 = \{ a_1 + [a_1^2 + 8 a_0 (K-1)]^{1/2} \} / 4. \qquad \text{eq. 11}$$

$$G_6 = a_0/G_7. \qquad \text{eq. 12}$$

The denormalized capacitances and resistances were calculated as above with equation 8 and

$$R_i = \text{ISF}/G_i , \qquad \text{eq. 13}$$

where i = integer index, using μ and ISF with f_o = 90 kHz.
The transfer function of the LPF is given by:

$$H(s) = \frac{Kb_0}{s^2 + b_1 s + b_0} \qquad \text{eq. 14}$$

where the variable gain, K, is set by R11/R10 + 1 ≈ 5. For a ripple width of 0.5 dB, b_0 = 1.516 and b_1 = 1.426. The dc offset of the filter is minimized by choosing

$$R11 = K(R8 + R9) \qquad \text{eq. 15}$$
$$R10 = K(R8 + R9)/(K - 1). \qquad \text{eq. 16}$$

R8 and R9 are determined in a similar fashion to the HPF by solving for the following conductances:

$$G8 = \{ b_1 + [b_1^2 + 8 b_0 (C4 + 1 - K)]^{1/2} \} / 2. \qquad \text{eq. 17}$$
$$G9 = a_0/G8. \qquad \text{eq. 18}$$

To make the radical in equation 17 positive, C4 was set to 4F. The denormalized capacitances and resistances were determined by equation 8 and 13, respectively, with fo = 100 kHz. The overall bandwidth of the BPF section is center about 95.2 kHz with an upper -3 dB frequency of 96.5 kHz and a lower -3 dB frequency of 94.3 kHz. Then Zt is AM demodulated to remove the carrier signal. This is accomplished by the classic diode-LPF series combination. To improve on the carrier frequency rejection, the typical passive LPF has been replaced by a VCVS Chebyshev active LPF. Design requirements included a maximum attenuation in the pass band of 0.5 dB (ripple factor, ε = 0.349) and a minimum attentuation in the stop band of 60 dB. The cutoff frequency is 9 Hz ($\omega c = 20\pi$) and the stop frequency is 30 Hz ($\omega s = 60\pi$). To obtain these features, a fifth order filter was required, as determined by solving for N (filter order) in equation 19 .

$$20 \log \varepsilon - 6 (N - 1) - 20 N \log \omega s/\omega c \geq 60 \text{ dB} \qquad \text{eq. 19}$$

Three active LPFs were cascaded, one first order stage, which included a gain of -6 (set by resistor R1), and two second order stages, both with a gain of one. The transfer function of each stage (H1, H2, H3) is multiplied to obtain the overall H(s) as:

$$H(s) = H1\ H2\ H3 \qquad \text{eq. 20}$$

$$H(s) = \frac{-K_0\ K_a b\ K_b b_2}{(s + b_0)\ (s^2 + a_1 s + b_1)\ (s^2 + a_2 s + b_2)} \qquad \text{eq. 21}$$

where K_0, K_a, and K_b are the gains of stages 1, 2, and 3, respectively. For a 0.5 dB Chebyshev filter, the coefficients are: b_0 = 2.863, a_1 = 0.351, b_1 = 1.064, a_2 = 0.947, and b_2 = 0.356. Using a similar normalizing/denormalizing procedure are above, the circuit components are determined as follows. The capacitors are normalized as C1 = C3 = C5 = 1F, C2 = 0.025 F, and C4 = 0.6 F. The conductances are calculated by using equations 22 - 27.

$$b_0 = G2/C1 \qquad \text{eq. 22}$$
$$K_0 = -G1/C1 \qquad \text{eq. 23}$$

$$G3 = \{ a_1 + [a_1^2 + 4 b_1 (C2 + 1 - K_a)]^{1/2} \} / 2 \qquad \text{eq. 24}$$

$$G4 = C2\, b_1/G3 \qquad \text{eq. 25}$$

$$G5 = \{ a_2 + [a_2^2 + 4 b_2 (C4 + 1 - K_b)]^{1/2} \} / 2 \qquad \text{eq. 26}$$

$$G6 = C4\, b_2/G5 \qquad \text{eq. 27}$$

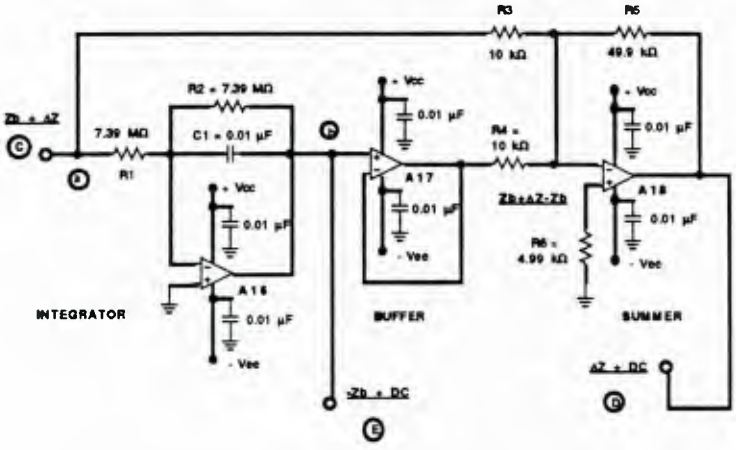

Figure 7. Separation of Zb (Baseline Impedance Signal) From ΔZ (Pulsatile Impedance Signal).

KEY

A16-17 : TL071N JFET Input Wideband Op Amp.
A18 : LF356N.

Features:
Continuous Integrator.: Matched valued resistors maintain identical DC offset amplitude at opposite signs at points "a" and "b." This ensures that ΔZ is centered about Zb with a small DC offset remaining.
f_c = 2.15 Hz, Time constant = 74 ms.
Amplifier Summer : Extracts ΔZ by removing Zb by simple subtraction.
Rc : Eliminates voltage offset by balancing impedance at input terminals of A18.

Capacitor and resistance values were denormalized using equations 8 and 13, respectively, for f_o = 10 Hz. The higher value capacitors (0.22 and 0.47 µF) are mylar type for better filter stability. To isolate ΔZ, the baseline impedance is removed by using a slow integrator (time constant (t = R1C1) = 74 ms) and an analog summing amplifier (see Figure 7). A16 is a continuous integrator with matched high value resistors at the negative input terminal and in the feedback loop. A continuous integrator features a dc "gain stop" resistor, R2, across C1 to reduce the integrator gain from the full open-loop value . In order to obtain such a long time constant, very large resistances were employed to prevent possible input failure by using a capacitance > 0.1 µF . Error from input bias current is minimized by the use of a high input impedance op amp and mylar capacitors. These resistors maintain identical dc offset amplitude of opposite polarity at points "a" and "b." This ensures that ΔZ is centered about Zb with a small dc offset. Integration over a relatively long time period acts to eliminate the pulsatile waveform while averaging Zt. Therefore, ΔZ drops out of equation 28 during the long term continuous integration.

$$Vout = -(1/R1C1) \int V_{in}\, dt \qquad \text{eq. 28}$$

where Vin is the voltage at point "a," referable to ΔZ + Zb and Vout is the voltage at point "b," referable to -Zb + dc. The limits of integration are from any arbitrary point in time to 74 milliseconds lat-

er. -Zb + dc is then summed with Zt in an analog summer to produce ΔZ + dc, as seen in equation 29.

$$V(\Delta Z + dc) = V(Zt)\,(R5/R3) + V(-Zb + dc)(R5/R4) \qquad \text{eq. 29}$$

Note that the voltages listed in equation 29 refer to their associated impedances. The gain of each input to A18 is -5 and R6 acts to eliminate offset voltage error by balancing the impedance seen by the input terminals of A18.

The negative dc offset that accompanies Zb is removed by a subtraction circuit with a variable positive voltage reference source, LM317, and is shown in Figure 8.

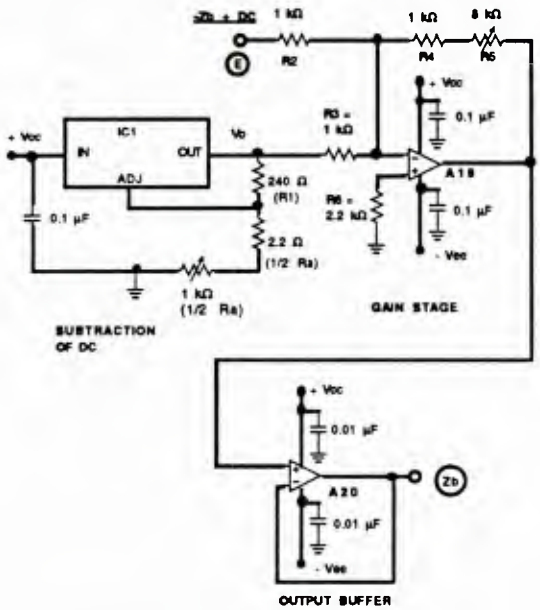

Figure 8. Remove DC From Zb (Baseline Impedance Signal), Amplification and Buffering of Zb.

KEY

A19-20 : LM741
IC1 : LM317 - Variable Positive Voltage Reference.

Vo = Output voltage from LM317:
Vo = Vref (1 + (Ra/R1))
Vref = Vo-Vadj. at terminals

. The output voltage of the LM317 (Vo) compensates for the negative offset according to equation 30.

$$Vo = V_{ref}\,(1 + Ra/R1) \qquad \text{eq. 30}$$

where Vref = Vo - Vadj; reference voltage equals the difference between the voltage at the output and adjustment terminals of the LM317. The subtraction circuit is an analog summer which produces an amplified voltage referable to Zb without a dc offset, V(Zb), whose value is determined by equation 31.

$$V(Zb) = V(-Zb + dc)(R4 + R5)/R2 + Vo\ (R4 + R5)/R3 \qquad \text{eq. 31}$$

Zb is then buffered for output for passage to other devices.

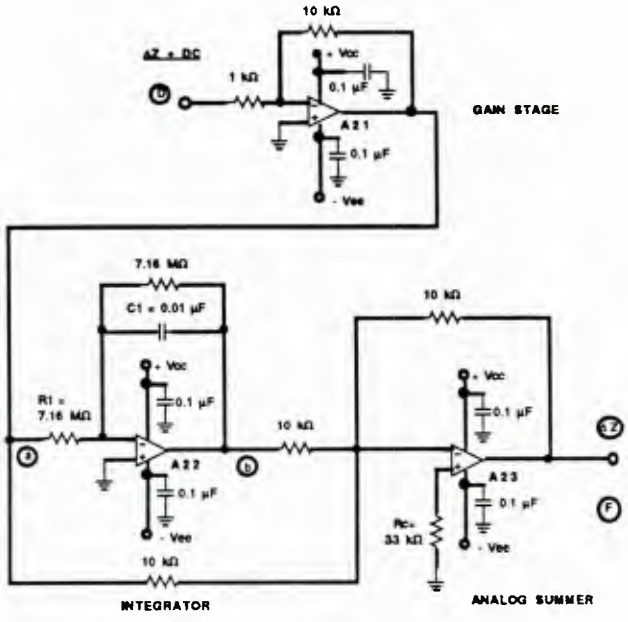

Figure 9. Separation of DC Offset From ΔZ (Pulsatile Impedance Signal).

KEY

A21 : LM318
A22,23 : TL071N

Features:
- Gain stage of 10 to boost size of ΔZ.
- Continuous integrator.: Matched valued resistors maintain identical DC offset amplitude at opposite signs at points "a" and "b." This ensures that ΔZ is centered about 0 V. f_c = 2.22 Hz, Time constant = 72 ms.
- Amplifier Summer : Extracts ΔZ by removing DC by simple subtraction.
- Rc : Eliminates voltage offset by balancing impedance at input terminals of A21.

The dc component that remains with ΔZ is also removed by a slow integrator and an analog summer in a circuit similar to that in Figure 9. The explanation accompanying the previous circuit is identical except that the voltage referable to ΔZ + dc is passed through an inverting amplifier with a gain of 10 and the time constant for this circuit is 72 ms (t = R1C1).

To increase signal-to-noise ratio, the pulsatile impedance signal is then low pass filtered using a Reticon© 7 pole-6 zero elliptic switched capacitor filter (RF5609A) (see Figure 10), which has a 75 dB stop band rejection and less than ±0.5 dB passband ripple. dc offset voltage is nulled by a voltage divider network between pins 1 and 7. Filter characteristics are controlled by an external clock circuit which is set to frequency $f$clk = 1200 Hz. The cutoff frequency, fc, is 0.1 $f$clk, or 12 Hz. The sampling rate is 50 fc, or fs = 600 samples/sec. The square wave clock is an RC comparator oscillator consisting of a LM319 high speed linear comparator whose frequency is set by $f$clk = 0.56/R1C1. This circuit produces an easily tuned, very accurate, stable square wave output. For accurate reproduction by the sampling system of the filter, no frequencies greater than fs/2 can be connected to the input of the filter. To insure this, ΔZ is first passed through an antialiasing second order VCVS Butterworth LPF.

The components of this filter are derived as above by using equations 14-18 using Butterworth coefficients b_0 = 1.0 and b_1 = 1.414 and a gain of 1. The cutoff frequency is 200 Hz. De-

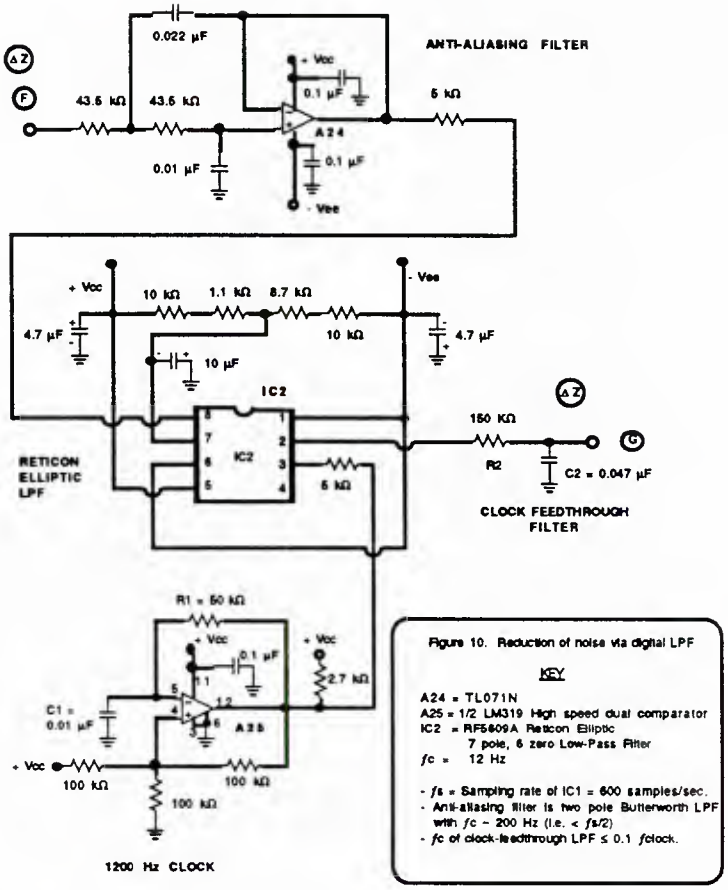

normalized capacitances and resistances are found using equations 8 and 13, respectively. To remove noise spikes generated by the clock, the filter output is passed through a passive R-C LPF, with a cutoff frequency $fc \leq 0.1\ fclk$. Therefore, $fc = 1/(2\pi R2C2) = 22.6$ Hz.

The processed ΔZ waveform is passed through a variable gain stage (Gain = 28 - 77) and buffered. This waveform is passed to a BNC connector for output to external recording or digitizing equipment. If necessary, ΔZ can also be inverted.

The waveform is then sent to a variety of recording devices. Data is stored onto FM tape, strip charts, or is passed to an automatic data acquisition system. One such system we have developed consists of the Macintosh Plus™ and a Micromint™ minicomputer. This system is an expanded refinement of an earlier Drexel Macintosh/Micromint system .

Figure 11. Averaged ΔZ With Indicies Explained

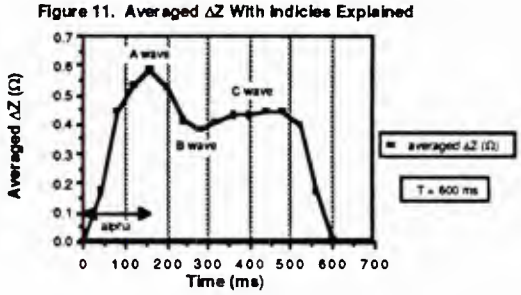

Figure 11 illustrates the waves or other components of the rheoencephalograph referred in the following discussion.

(2). Animal Experiments

To demonstrate the development of the REG device, the results of two experiments performed on a dog and a rabbit in the laboratory at 1 g will be briefly described. Besides the obvious anatomical differences, canines and rabbits differ from each other and humans in their respiratory and heart rates and mean arterial blood pressure (see Table 1). These differences must be kept in focus when comparing the REG waveforms among different species. For all animals tested, ΔZ retained its pulsatile nature at a heart beat coincident rate. All ΔZ waveforms contained an A wave. However, the form of the descending branch of ΔZ was quite variable. The effects of respiration on REG signals were quite evident in the animal studies.

Dog and rabbit facial muscles are highly vascularized and highly moveable. One might expect that the extracranial component of the REG would be higher in animals as compared to man, though this was not specifically determined. References in the literature detailing REG studies using animals are few in number and are often not performed due to the differences in anatomical geometry and circulation.

One of the major difficulties we had during our animal experiments was electrode motion artifact. While the animals were sedated, they often moved their facial muscles while unconscious, thereby producing artifacts in the REG waveform. A variety of electrode types were used, including Beckman EEG needle electrodes, stainless steel surgical needles, acupuncture needles, alligator clips, and surface disk ECG type electrodes. Motion artifact remained an obstacle for all recordings regardless of the electrode types and whether recordings were obtained superficially or by piercing the skin.

	Rabbit	Dog	Human
Respiratory Rate (/min)	36.8±10.6	28.2±3.3	12
Heart Rate (bpm)	246	155	65
Mean Arterial Blood Pressure (mmHg)	82-133	113±2.7	100
Brain weight (gm)	8.2-10	76-81	1500

Table 1. Comparison of resting physiological data among rabbits (New Zealand White), dogs (beagle) , and humans .

The first experiment employed an early version of the REG instrument in August of 1986 and used a 25 pound mongrel dog. The dog was anesthetized and intubated. Physiological recordings included ECG, aortic pressure, descending aortic flow, and ΔZ. Stainless steel needles were used as electrodes and were inserted into the scalp bitemporally. The signal was of low amplitude and quite variable, specially on the descending branch. When the exhalation port of the respirator was temporarily closed and intrathoracic pressure increased, the A wave of the ΔZ waveform became much more sharply defined and the multiple inflections after the C wave were markedly dampened and very close to the baseline. This occurred about 13 seconds after the exhalation port of the respirator was blocked. By this time the ECG contained T wave inversions, indicating that the heart was distressed due to oxygen insufficiency . Aortic pressure had dropped from a mean of about 125 mmHg to 60 mmHg. Unfortunately, aortic flow went offscale during this functional test. Approximately 16 seconds into the test the amplitude of the A wave became too small to distinguish it from the rest of the ΔZ waveform. After 20 seconds, the dog's heart began to recover and aortic flow increased approximately four times over the resting levels (peak systolic flow of 0.6 L/min vs 0.16 L/min). The A wave became exaggerated and the descending portion of the waveform became elevated with clearly defined B and C wavelets. In fact the amplitude of the C wave was greater than the A wave. This may be indicative of increased blood outflow. This difference

persisted for five seconds until peak systolic aortic flow reduced to 0.5 L/min. When the expiration port was opened , aortic pressure and flow returned to pretest levels, as did the REG. Peak systolic aortic flow recovered to 0.3 L/min when ΔZ returned to unstressed levels. Interpretation of these waveforms is complicated by the large swings in hydrostatic pressure this test creates.

Another procedure (December 1987) involved a five pound rabbit. Physiological recordings included oxygen tension measurements, using recessed cathode oxygen microelectrodes, ECG, ΔZ, and Zb. Respiration patterns were apparent by looking at the wide baseline swings of the ECG. Unstressed ECG, ΔZ, and Zb recordings on an anesthetized animal (ketamine and rompun) were made prior to any surgical intervention. EEG needle electrodes placed fronto-occipitally were used to record REG signals. The surgical procedure included reflecting the skin back over the skull and a burr hole was bored mid-sagittally between the eyes and ears, exposing the cerebrum. The carotid arteries were also exposed. Measurements were taken with the skull exposed and with and without the carotids occluded. With the skull open the effect of tidal changes in intrathoracic pressure with respiration on the intracranial pressure of the exposed brain was manifested by a swelling of cerebral tissue up out of the hole upon exhalation. B and C waves were much more sharply defined with the skull exposed as compared to the unstressed measurements. In fact the B wave was usually obscured prior to surgery. During carotid occulsion, most of the ΔZ waveforms were saturated. However, after the occulsion was released, the magnitude of ΔZ was slightly reduced (≈ 16%). This decrease in impedance corresponds to the inrush of blood back into the cranial space from the carotids. The effects of respiration on Zb were very evident in that the baseline swings in the ECG referable to respiration were accompanied by similar excursions in Zb, though the signals were 180° out of phase. During occlusion, the oxygen tension fell from 37 to 22 mmHg at a disappearance rate of -4 mmHg/sec. This rate can be compared to a similar experiment (Nair, P.K., Buerk, D.G., and Halsey, Jr., J.H.: "Comparison of Oxygen Metabolism and Tissue pO_2 in Cortex and Hippocampus of Gerbil Brain." Stroke, 18: 616, 1987.). They report that the cerebral metabolic rate for oxygen (CMRO2) was 8.3 ml O2/100 gm/min in the cortex and the disappearance rate was -23 mmHg/sec. Even though the CMRO2 for rabbits is about half that of gerbils, the disappearance rate appears to be somewhat too low. This result indicates that complete occlusion of the carotids was not attained.

This was a demonstration experiment to determine the potential difficulties involved with simultaneous REG and oxygen tension measurements. There was apparently no electrical interference between the two measurement techniques. It is difficult to make conclusions based upon an experiment in which there was only one subject. However, given the circumstances of the experiment, the results are not inconsistent with the case in which circulation to the brain is arrested while oxygen consumption proceeds at a normal rate.

(3). Human Studies

The REG has been constructed and has undergone initial testing in both normal and simulated military stress environments. The REG has withstood stresses of at least +14 Gz. Measurements on human subjects have been taken at extremes of +8 Gz and -1.5 Gx. One of the most notable features of the ΔZ waveform is its highly variable nature. Automatic data processing must be used very carefully in order to trust its evaluations. Otherwise, data processing can be done by hand with certain, though more tediously obtained, results.

The data from the first centrifuge experiment, CE1, was processed using the digital signal processing equipment at NADC. Of the data recorded onto FM analog tape, only the ECG, pulsatile REG, infrared plethysmograph, and the baseline REG were readable. Data was organized into files consisting of 7 - 8 heartbeats (5.76 seconds, with each data point representing 5 msec). The range of the data was ±5 volts with a 12 bit resolution. Acceleration onset and offset were determined by using the strip charts and the audio recording of the subjects, the centrifuge operator, and the flight deck personnel.

The form of the ΔZ was very variable due in part to the existence of muscle and motion artifact. The simplest method for extracting the random noise out of a repetitive waveform is to average it. Six waveforms were averaged to obtain a template, representative of unstressed and stressed

waveforms for ECG, ΔZ, and IRP. As a fiducial point to commence averaging, the R wave of the ECG was chosen. The R wave was detected via an amplitude threshold method in which the maximum of the total record of ECGs was calculated (a 5.76 second slice of time). An R wave was "captured" if the amplitude of the waveform was 70% of the maximum. Once detected the algorithm skipped the next five data points to avoid registration of false positive detections before searching for the next R wave. Heart rate (HR) varies under the effects of acceleration. As acceleration increases, so does heart rate. During protracted runs, bradycardia can occur to some extent. The timing of the latter appears to coincide with the onset of cardiovascular (CV) compensation . Since the HR was variable, after obtaining the template magnitude, the period of the shortest was chosen as the length of the template. For each record, the lengths of the six intervals, the length of the shortest, the maximum amplitude of the R wave, and HR were calculated. Both averaged and raw ECG signals could be saved to disk.

ΔZ and IRP were processed in a similar manner to the ECG. The maximum value of the A wave, ΔZmax, was also calculated via a threshold detection algorithm. The threshold was set at 50% of the largest peak in the record. Once detected the algorithm skipped the next 25 data points to avoid registration of false positives prior to searching for the next ΔZmax. Analogously, the threshold for IRPmax was set at 30% of the largest peak in the record and the next 80 points were skipped. The periods of ΔZmax-ΔZmax and IRPmax-IRPmax were calculated and compared to the R-R intervals. Theoretically, the timing of the R-R interval and the ΔZmax-ΔZmax period should be the same. By aligning the averaged ΔZ waveform to the start of the averaged ECG signal, i.e. the R wave, pulse wave delay is simply the time from the beginning of the record to ΔZmax. Once the averages have been obtained, the waveforms can be analyzed in both the time and frequency domains. Correlations can be performed to determine the fit of the averaged as compared to the raw signal. The timing relationships between the ECG and pulsatile waveforms can also be verified via cross correlations.

Power spectral density functions (PSD) can be generated to determine the frequency content of the various signals. We can compare these spectra to each other and we can determine the effect of increasing acceleration load on the PSD of these waveforms. The analysis of the data obtained during CE1 was centered on the best available data, i.e. from subjects S1 and S5. For this analysis, data used were from gradual onset runs (GOR) and rapid onset runs (ROR). For S1, these started at a +1.03 Gz level and for S5, these started at a +1.8 Gz level. Analysis of IRP signals proved fruitless due to the low amplitude and lack of easily definable peaks. Threshold detection for this waveform was clearly not the best approach. Zb contained a rather large dc offset that obscured the low level changes in Zb seen in subsequent experiments. However, upon careful examination of the strip charts, Zb changed in magnitude and followed the +Gz trend, indicating a shift of blood out of the head. The magnitude of these changes with respect to those at a 1 g level was not statistically significant.

One expects that under a +Gz load, cephalic fluid volume should be reduced according to the hydrostatic column theory. This reduction in volume ought to accompany an increase in impedance which would be reflected by an increase in the amplitude of the A wave. Cardiovascular compensation can occur after about ten seconds of acceleration exposure, though the timing does depend on the onset rate and level of acceleration stress. Comparison of the effects of acceleration during GOR exposures to S1 and S5 on A wave amplitude were inconclusive. For both individuals the A wave initially decreased as acceleration approached +1.8 Gz. A wave amplitude for S1 then increased until the acceleration was offloaded. In the case of S5, however, A wave amplitude oscillated. There was certainly enough time for compensation to occur though it is difficult to conclusively state that from A wave analysis alone.

Another limitation of the automatic data processing results was discovered when analyzing the difference in time periods between the R-R and the ΔZmax-ΔZmax intervals. When comparing the the values obtained by the threshold detection algorithm, there was a significant difference between the two intervals for both S1 and S5 (determined by a paired t test, $p < .009$ and $p < .002$, respectively). However, hand analysis of the strip charts proved that the intervals were virtually the same and that as heart rate increased during acceleration, the ΔZmax-ΔZmax period decreased (determined by a paired t test, $p < .418$ and $p < .170$, for S1 and S5 respectively). No

such problem was found in the determination of the pulse wave delay or "delta delay," (ΔD). As found by Hrebien (Hrebien, L.: Pulse Wave Delay for +Gz Tolerance Assessment. NADC Report No. NADC-86140-60, 1986) in doppler ultrasound studies , there was a similar relationship between the time of the occurrence of the R wave and the subsequent peak of the A wave and the imposition of a high +Gz load. As acceleration increases, the delay also increases linearly. ΔZmax occurs approximately 320 msec after the "R" wave at +1 Gz and about 360 msec after the "R" wave at +3 Gz. These values are somewhat higher than those reported by Hrebien but the acceleration profiles were also quite different. The linear regression equations are:

$$S1:\ \Delta D = 0.31 + 0.23\ Gz;\ R^2 = 0.89\ , \qquad \text{eq. 32}$$

$$S5:\ \Delta D = 0.25 + 0.05\ Gz;\ R^2 = 0.80\ . \qquad \text{eq. 33}$$

In the course of examining the frequency content of the signals, several interesting features became apparent. The frequency content for GORs is shown in Tables 2 and 3. Under acceleration stress the frequency content of ΔZ changed whereas the frequency content of both the ECG and the IRP remained the same. Waterfall plots of the effect of increasing acceleration stress on frequency content were constructed. This alteration occurred even though heart rate only rose, during the onset to plateau periods, from 88.9 to 108 bpm (S1) and from 86.3 to 101.7 bpm (S5). The most notable change seen under a +Gz load included an increase in frequency content of the primary lobe at +3 Gz (from ≈ 2 Hz to 4 Hz, for S1, to 5.8 for S5) and a reversal from minima to maxima at +3 Gz at ≈ 9.5 Hz. There was another change from an unstressed frequency maxima to a stressed frequency minima, though these occurred at different frequencies (S1: 6.4-6.8 Hz and S5: 8.6 Hz).

+Gz	FREQUENCY (Hz)	MAGNITUDE(dB)	MAXIMA/MINIMA
any	2 - 2.6	0 - -1	maxima
3	2 - 4	0	**maxima**
any	4 - 4.5	0 - -5	maxima
any	7.2 - 8.2	-11 - -20	maxima
any	10.6 - 11.6	-20 - -31	maxima
any	5.4 - 7 -	12.5 - -34	minima
any	9 - 10.6	-22 - -34	minima
< 3	6.2 - 6.4	-12.25	maxima
3	6.4 - 6.8	-21.5	**minima**
< 3	9.4 - 10	-30.1	minima
3	9.6	-14.5	**maxima**

Table 2. Subject S1: ΔZ frequency content changes with increased +Gz load. Reversals from maxima to minima and vice versa at +3 Gz are shown in bold face. Runs were gradual onset.

In an attempt to discover whether or not the changes in frequency content outlined above are related to the time domain change in the ratio α/T, cross correlation analysis (Rxy) was performed. Frequency content data could be described on the basis of the peak of the fundamental frequency band (f) or the -3 dB (f_{-3dB}) decline from that fundamental. Plots of f and f_{-3dB} with respect to rising and falling levels of acceleration, expressed in +0.1 Gz steps, for subjects S1 and S5 were constructed. In these α/T is expressed as 10 α/T for a clearer plot. Since f consists of a band of frequencies, frequency content is expressed as two curves. 'Low peak f' refers to the low frequency bound of f and 'high peak f' is the corresponding upper bound. Plots of these and f_{-3dB} are similar in appearance. Since f is characterized by a range of frequencies, a cross correlation is difficult to determine and weight properly with such a continuum of values. Therefore

a cross correlation was performed between f_{-3dB} and 10 α/T.

+Gz	FREQUENCY (Hz)	MAGNITUDE(dB)	MAXIMA/MINIMA
any	1.8 - 2.4	0	maxima
< 3	4 - 5.4	-15.5	minima
3	1.8 - 5.8	0	**maxima**
any	5.4 - 6.2	-7.75	maxima
any	10.6 - 11.4	-17.5	maxima
any	6.4 - 6.8	-19.25	minima
3	9.4 - 9.8	-16.5	**maxima**
< 3	9.4 - 9.8	-30.4	minima
3	8.6 - 9.2	-25.9	**minima**
< 3	8.6 - 9.2	-18	maxima

Table 3. Subject S5: ΔZ frequency content changes with increased +Gz load. Reversals from maxima to minima and vice versa at +3 Gz are shown in bold face. Runs were gradual onset.

To calculate Rxy, the sum of the dot products was taken between all points of f-3dB , i.e. the kernal, and each point of the 10 α/T waveform (t10α/T). This included a total of 2N-1 points, where N is the number of data points. Rxy ranges from -N to N. If the correlation was perfect, the result would be the same as the kernal squared, i.e. each data point matches between the kernal

Figure 12. Correlation Function: -3dB vs alpha/T : Subj. S5

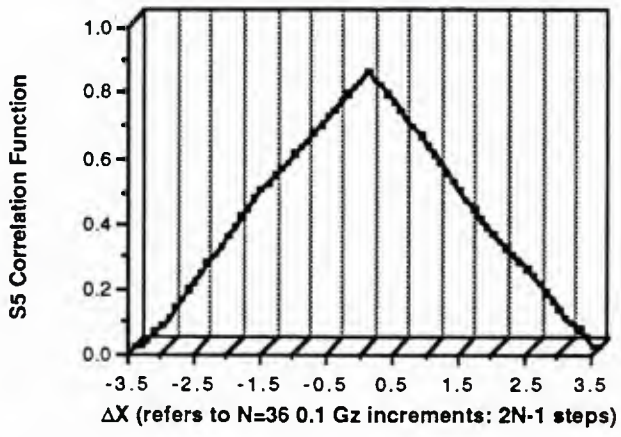

and f-3dB. Therefore, the sum of the dot products was normalized to 1.0 by dividing each point in the sum by the sum of the squared magnitudes of the kernal points.

A perfect positive cross correlation function would resemble an impulse function with a value of 1.0 positioned at the center of the function, i.e. $R_{xy}(0)$. Rxy for S5 ($R_{xy:S5}$) is plotted (e.g. figure 12) . While these functions do not indicate a perfect positive correlation as defined above, they do show that f_{-3dB} and $t_{10\alpha/T}$ are probably (in the statistical sense) weakly correlated with $R_{xy:S1}(0) = 0.64$ and $R_{xy:S5}(0) = 0.84$. Since there is no "figure of merit" for nonlinear cross correlation and the fact that the bulk of the power of the signal should be at $R_{xy}(0)$, the area under the Rxy curve was calculated and compared to the area bounded by one standard deviation (±1 s) centered about $R_{xy}(0)$. Each Rxy waveform was fitted to a fourth order polynomial (equations 34 and 35). Equations 36 and 37 were used to determine the relative amount of the waveform that was within ±1 s, i.e. 68% of the distribution.

$$R_{xy:S1} = 0.581 + 0.024x - 0.073x^2 - 0.002x^3 + 0.002x^4$$

for $-N \le x \le N$; $R^2 = 0.994$ eq. 34

$$R_{xy:S5} = 0.743 - 0.014x - 0.118x^2 + 0.001x^3 + 0.005x^4$$

$$\%S1 = 1 - \frac{\int_{-4}^{4} R_{xy:S1}\,dx - \int_{-2.5}^{2.5} R_{xy:S1}\,dx}{\int_{-4}^{4} R_{xy:S1}\,dx} \quad \text{eq. 36}$$

$$\%S5 = 1 - \frac{\int_{-3.5}^{3.5} R_{xy:S5}\,dx - \int_{-2.2}^{2.2} R_{xy:S5}\,dx}{\int_{-3.5}^{3.5} R_{xy:S5}\,dx} \quad \text{eq. 37}$$

for $-N \le x \le N$; $R^2 = 0.993$ eq. 35

It was found that 92.8% of $R_{xy:S1}$ lies within ±1 s of $R_{xy:S1}(0)$ and 88.1% of $R_{xy:S5}$ lies within ±1 s of $R_{xy:S5}(0)$. These values tend to support the validity of the cross correlation, assuming that equations 34and 35 are good representations of the actual curve.

Centrifuge Experiment 2 (CE2)

Following the mixed success of automatic data processing for experiment CE1, experiment CE2 was processed by hand, with the help of automated statistical packages. It is important to point out at the onset of this discussion that demonstration of statistical significance does not imply clinical or experimental significance. Statistical significance can merely determine whether or not events occur due to chance alone. In this study, we were able to investigate the effects on the REG waveforms of a common technique to increase +Gz-tolerance, i.e., reclining the seat back from the vertical. Of most interest in this study was the effects of changing seat-back-angle (SBA) under acceleration on Zb while the subjects were seated in a PALE (pelvis and legs elevated) seat. Results from this experiment were presented at the 1988 Annual Scientific Meeting of the Aerospace Medical Association.

As a +Gz load is applied to a subject, there is a fluid shift out of the head down towards the abdomen and large capacitance veins of the legs. If Zb does indeed reflect the bulk movement of blood in and out of the head, then one should see a change in inflection in the waveform in conjunction with applied stress. Under 1 g conditions, Zb remains fairly stable without much change

in the overall voltage level. With the application of stress, Zb decreases along with the increasing +Gz load during a "relaxed" run. A relaxed acceleration exposure usually consists of a subject wearing a standard anti-G suit, which may or may not be inflated, a flight harness, and the subject does not perform an anti-G straining maneuver. In fact, as acceleration increases so does the magnitude of change in Zb. As the +Gz load is lifted, Zb returns back to a consistent level that is approximately the same as the prestress levels. Prior to attaining this level, there is an overshoot in the waveform. This overshoot is consistent with the onrush of blood back into the head and increased blood pressure that occurs to compensate for the temporary acceleration induced loss in volume. Signal overshoot has also been seen in doppler ultrasound velocimetry recordings under a +Gz load performed in the human centrifuge at NADC. This indication of increased cephalic circulation and therefore ability to withstand higher acceleration stress occurs at an angle which is consistent with the studies done by Harald von Beckh at NADC in the 1970's . In that study he reported an increase in +Gz-tolerance at a SBA of 45°. During experiment CE2, the average SBA in which there is an indication of the reversal of outward blood flow from the head is 49.25°. In Table 4, a summary of the SBA, Gz level and onset rate for ramp-type centrifuge runs at the point of inflection of Zb is presented. Changes in output voltage referable to Zb as acceleration load is increased and decreased, %ΔZb, SBA, and time from acceleration onset were also noted. Upon offloading of the stress, the Zb waveform demonstrates a similar overshoot and subsequent return to prestress levels as seen in relaxed runs. These changes in Zb may allow us in future studies to use REG waveforms as an aid in determining the efficiency of anti-G protective devices.

ONSET RATE	+Gz at Zb INFLECTION	SBA
+2.3 Gz/sec	6.8	50°
+2.3 Gz/sec	6.8	48°
+0.5 Gz/sec	5.5	54°
+0.5 Gz/sec	4.7	48°
+0.5 Gz/sec	4.6	48°
+0.1 Gz/sec	4.8	51°
+0.1 Gz/sec	4.6	49°
+0.1 Gz/sec	4.4	46°

Table 4. +Gz and seat-back-angle (SBA) at which there is a change in inflection of Zb during ramp-type acceleration exposures in experiment CE2.

Centrifuge Experiment 3 (CE3)

Circuitry improvements in the REG device permitted the collection of the best ΔZ and Zb data to date during experiment CE3. Specifically, enough data to characterize the magnitude and timing changes in impedance signals under acceleration stress was collected under relaxed and straining conditions.

Baseline REG (Zb)

In the REG device, Zb is derived from a hardware combination of subtraction from and a slow (i.e. a long time constant) integration of ΔZ. Measurements are expressed as a percentage change in baseline from unstressed (i.e. 1 g) to a high +Gz load environment. As mentioned previously, as acceleration load increases, so does the magnitude of the change in Zb. Zb data from four of the subjects was used to describe the change in Zb with respect to unstressed (+1.03 Gz) values taken five seconds prior to acceleration onset. These values were expressed as a percent change (%ΔZb), with the unstressed levels arbitrarily set to zero. According to the hydrostatic column theory, CV compensation can occur after about ten seconds of acceleration exposure, assuming that the onset rate was not so great as to overwhelm the CV system, which leads to loss of consciousness. Therefore, readings were taken five seconds prior to acceleration onset, during the two second onset, during the first, second, and third five second periods at plateau, during

the two second acceleration offset, at the peak of the overshoot, and at the point of baseline recovery. The average values of %ΔZb at +2.5 to +4.5 Gz for four relaxed subjects are presented in Table 5. Also in Table 5 are values for runs that were stopped because the subjects' peripheral vision closed down to a 60° forward visual cone (labelled PLL, peripheral light loss, in the table).

	Time Into Run From +Gz Onset						
+Gz	0-2s	2-7s	7-12s	12-17s	17-19s	peak	settle
2.5	-.222	-.200	-.247	-.295	-.148	-.05	-.122
3.0	-.142	-.152	-.186	-.22	-.062	-.006	.026
3.5	-.291	-.300	-.379	-.416	-.009	.129	.05
4.0	-.516	-.571	-.572	-.611	-.186	.121	.008
4.5	-.367	-.509	-.547	-.556	-.184	.184	.084
PLL	-.451	-.634	-.621	x	x	x	.053
AGSM	-.180	.132	.266	.348	.214	.440	.040

Table 5. Percent change in Zb with respect to +1.03 Gz levels during various points throughout the ROR. See text for explanation.

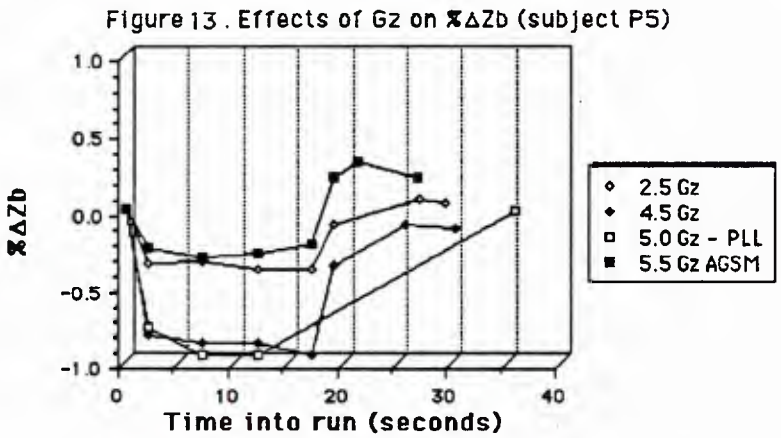

This endpoint occurred at an average level of +5.17 Gz after approximately ten seconds at plateau. The last line in the table, labelled AGSM (anti-G straining maneuver) , are the values of %ΔZb obtained while the subjects performed an L-1 maneuver. These values are taken during the forced exhalation period of the straining maneuver. A plot of %ΔZb with respect to run time and acceleration level is presented in Figure 13.

From this data several observations can be made. As acceleration stress increases, so does the magnitude of %ΔZb. Upon offloading of acceleration stress, there is an overshoot corresponding to the influx of blood reentering the head due to the effects of CV compensation. The relative amount of this overshoot tends to rise with increasing acceleration load, which corresponds to the increased amount of CV compensation necessary to restore the neural tissues to normal conditions. After the run, %ΔZb returns to the previous unstressed level within approximately 10%. This change in Zb level indicates that the subject's CV system has readjusted and

blood flow has been restored.

One way analysis of variance (ANOVA) was performed on %ΔZb with respect to acceleration load to discover if a significant statistical relationship exists between the baseline impedance and increasing acceleration level at plateau. We can see that while is there some biological variability in the data, i.e. %ΔZb at +2.5 Gz is greater than at +3 Gz, the relationship between increasing acceleration load and rising %ΔZb is highly significant (see Table 6).

Source	Sum of Squares	dof	Mean Squares	F	Prob>F
between +Gz	.439	4	.110	34.7	.0001
Error	.048	15	.003		
Total	.487	19			

Table 6. One way ANOVA comparing percent difference in the averaged baseline impedance with respect to +Gz level. dof = degrees of freedom.

Our data would seem to indicate that %ΔZb during straining is different from relaxed runs. The fact that at two seconds into the run no difference is apparent is probably due to inefficient straining technique during acceleration onset. Two tailed paired t tests were performed comparing relaxed runs (all grouped together) with straining runs. These tests were performed for each time period during plateau. As expected, at two seconds, the difference was insignificant ($p<0.12$) while at plateau the difference between the means was highly significant ($p<0.005$). One would like to be able to predict the onset of a PLL terminated run from the previous run time performance. Again, two tailed paired t tests were performed to judge the significance between the means at +4.0 and at +4.5 Gz with the PLL terminated run. These results were somewhat confusing due to the biological variability inherent in the data. The magnitude of %ΔZb values, while close, are greater at +4.0 than at +4.5 Gz. Therefore, while comparison between PLL and +4.0 Gz runs proved to be insignificant ($p<.736$), the results between PLL and +4.5 Gz were significant ($p<.026$). More data needs to be obtained to show that this reduction in %ΔZb prior to PLL runs is due to subject variability or is a consistent indication of potential cephalic circulation compromise. Therefore, this measure gives a good indication of the relative state of the cephalic circulation with increasing acceleration load and shows that straining is indeed an effective means to increase cephalic blood flow.

Effects Of Straining On Zb

During the performance of an AGSM, such as the L-1, there are very definite changes in the form and level of Zb that can be used as a gauge to aid in the evaluation of the effectiveness of the respiratory portion of the AGSM. The form and reference points for the straining Zb waveform are as follows:

1. I wave: Following a relatively flat or slightly sloped period corresponding to the forced expiration portion of the maneuver, there is a rise, the I wave, corresponding to the rapid expiration immediately preceeding the inhalation phase (the "KAH").
2. II wave: Next is a depression that corresponds to the first part of the rapid (< 30 sec) inspiratory phase, the II wave.
3. III wave: The second part of the inspiratory phase including the beginning of the forced expiration and muscle tensing is manifested by a large peak, the III wave, that corresponds to the "HOOK."
4. IV wave: This is a relatively flat portion of the curve that corresponds to the forced expiratory phase of the L-1.
5. Strain amplitude: The difference between the minimum of the II wave and the peak of the III wave gives a relative indication of the strength of the strain during the breath exchange portion of the AGSM.

6. Strain duration: This is measured from the peak of the I wave to the end of the III wave. An indication of the speed of the air exchange is evident from this measure. Ideally, this takes about 0.5 seconds .

7. Strain period: Measured between two I wave minima, this indicated the length of time the entire maneuver takes. Ideally, this should take three seconds .

In order to compare the effects of straining on bulk movement of blood under acceleration, one can compare Zb levels when relaxed under stress to IV waves when performing an AGSM.

By studying the Zb traces one can determine the speed of air exchange, relative strength of the respiratory effort, and the length of the strain. As an example, during the SACM (simulated aerial combat maneuver) phase of CE3, as time progressed during the runs and the subjects started to tire, some subjects exhibited some or all of the following responses: the straining period (I wave - I wave interval) decreased, strain duration (i.e. speed of breath exchange) lengthened, and the top of the strain amplitude wave (III wave) decreased in magnitude and flattened. Clearly, exhibition of these trends would indicate that the effectiveness of their straining technique was diminished. However, while straining amplitude and period both declined as SACM time increased, strain duration either lengthened or shortened depending upon the individual. The amount of straining effort an individual produces in the centrifuge, however, depends in large part to their level of motivation. During these trials, blood lactate measurements were made before and after SACM runs in order to determine whether subjects were engaged in anaerobic metabolism. These indicated that some subjects expended much more energy than others. It was difficult to determine for most of the subjects who truely reached a fatigue end point.

Therefore, while these changes in Zb are indeed promising and worthy of future investigation, more data needs to be obtained from a group of well trained clearly motivated individuals to reduce the variablity seen in these indicies, specially strain duration. Further, in order to gain a complete assessment of straining effort, electromyographic recordings of the arms, legs, and neck muscles are needed to complement the Zb respiratory information.

Once the additional information has been attained and baseline values and trends are known, may be possible to employ the REG as a training aid in the instruction of effective AGSM techniques in a noninvasive unobtrusive manner. Currently, one can monitor AGSM performance by measuring intrathoracic pressure by using an intraesophageal balloon. As one might imagine, it is difficult if not impossible to persuade volunteer subjects to use such a device.

E. Conclusions and Observations for Future Development

At the same time that the specific project goals have been achieved, many new insights have been gained into the general problem of physiologic monitoring under conditions of gravitational stress. We have found that enhancements in the acquisition of the REG signal have not necessarily made interpretation of the REG a simpler task. In fact, separation of the fast and slow components permits study of the pulsatile component in greater detail which leads to new complexity. When electrical impedance plethysmography is used to determine blood volume in the finger, leg, and forearm, to measure stroke volume in the chest , and pulse monitoring at the nasal septum, interpretation rests on the relatively simple assumption that, at any instant, the impedance change depends only upon the movement of blood into and out of the segment. Often the evaluation of flow can be further simplified by occlusion of the outflow path - as in venous outflow plethysmography.

Measurement of cranial impedance plethysmography is rather more complicated. For example, respiratory maneuvers not only induce baseline impedance shifts (i.e. Zb), but also introduce significant changes in the form and magnitude of the pulsatile component. We believe this arises from the interplay of blood circulation with shifts of cerebrospinal fluid (CSF). Unlike the limbs which can simply expand to accommodate volume changes, the brain resides in a rigid bony case and the CSF moves in and out of the head with changes in blood volume and external pressure (application of +Gz). Since the CSF is more conductive than blood, its volume changes have an important effect upon the REG signal.

Although the more complex and detailed view of the cephalic circulation which rheoencephalography affords requires a more systematic and sophisticated approach to analysis and interpreta-

tion, it also provides the opportunity to explore additional physiologic factors which may be playing significant and possibly even critical roles in the body's response to G stress.

Early in the development of aerospace physiology, the effect of +Gz on hydrostatic pressures in the circulatory system was formulated. Since that time, a major emphasis in dealing with the problem of peripheral light loss (PLL) and loss of consciousness (LOC) under +Gz, has been concern with maintenance of blood pressure and "forward" flow in the cerebral circulation. There is no doubt of the importance of such blood flow in the long term homeostasis of the central nervous system; however one may speculate that, over the periods of interest in preventing PLL and LOC, consideration of additional factors such as cephalic blood volume, "tidal" blood flow especially during G-protective maneuvers, and the general economy of oxygen distribution in neural tissues may be of comparable and even critical importance.

Among tantalizing observations in the area of +Gz tolerance may be found the following: (a) Respiratory maneuvers found to be helpful in postponing PLL and LOC in the short run are of a general nature that is detrimental to circulation in the long run. (b) The onset of PLL and LOC (in common with syncope at 1G) seems rather sudden to be explained by loss of flow alone. (c) Net negative blood velocities, when measured by the Doppler ultrasonic method, have been observed in the superior temporal artery for extended periods of time under +Gz stress without significant decrease in pilot performance. Insight into these observations is aided by consideration of some basic physiologic features of neural tissues. These tissues, including the retina and brain, have closely regulated but barely adequate blood circulation to supply nutrients (oxygen, glucose, etc) and remove waste - in contrast with organs such as skin, gut, and kidney whose abundant blood supplies reflect their circulatory interface function. Neural tissue comprises only three percent of body weight while receiving about 15% of the cardiac output and consuming about 25% of the oxygen. In the retina and in neural grey matter, oxygen consumption can be as high as 12 ml/100gm/min. By comparison with cardiac and skeletal muscles (having a similarly high oxygen extraction fraction), neural tissues lack an "on-board" oxygen buffer such as myoglobin. In the brain, oxygen is used only in the "terminal respiratory chain" of enzymes for oxidative phosphorylation in the mitochondria, i.e. ATP synthesis. This process is usually limited by the supply of ADP and inorganic phosphate rather than oxygen tension. Oxygen uptake by mitochondrial suspensions will continue until the local partial pressure of oxygen falls to 0.1 mm Hg. (Honig, C.R.: Modern Cardiovascular Physiology. Little Brown & Co, Boston, 1981). Therefore, when oxygen supply becomes limiting, it is because the volume or mass of oxygen has been exhausted. Oxygen consumption in the brain is 40 - 50 ml/min. There is only 2.8 ml of oxygen dissolved in the tissue. The 75 ml of blood in the cerebral circulation contains about 15 ml of oxygen, mostly combined with hemoglobin. Therefore the hemoglobin in blood is the major oxygen buffer for the neural tissues. In our view, PLL and LOC under +Gz are caused not only by interruption of blood flow to the head, but also by removal of the major proportion of available oxygen. This view is consistent with observations of the retinal vessels under direct ophthalmoscopic observation using fluorescein as an indicator. During +Gz not only is there a total cessation of pulsatile flow but an apparent backward flow of fluorescein dyed arterial blood from distal ophthalmic artery towards the carotid system. At offset of gravitational stress, the dye then returns to the ophthalmic artery and then is cleared from the arterial system (Leverett, S.D.: Aerospace Physiology and Medicine in Medical Engineering (C.D. Ray editor) Chicago, Year Book Medical Publishers. p 827, 1974.) Thus the benefits, during the short term, of G protective respiratory maneuvers may arise from "tidal" replacement and redistribution of the blood rather than actual net forward flow.

To the extent that these speculations are applicable, three suggestions emerge: (1) The effects of +Gz on the oxygen availability to neural tissues as well as benefits of G protective maneuvers will be reflected, in part, in cephalic blood volume changes (plethysmography). (2) Studies relating to G tolerance and protection should consider other aspects of the oxygen buffering of neural tissue by blood including hemoglobin concentration, and the allosteric effects of such substances as 2DPG concentration, carbon monoxide, etc. (3) Mathematical modeling for simulation of G effects on PLL and LOC should account for distribution of oxygen supply as reflected in cephalic blood volume changes and related molecular and cellular factors of the oxygen economy.

A natural outcome of these investigations will be a more "holistic" view of monitoring under G stress. Rather than using a one-dimensional approach, an array of non-invasive and (relatively) non-intrusive physiologic methods and behavioral tasks can be applied to humans. At the same time, more invasive studies in experimental animals can be used to validate the underlying models and assumptions (see figure 14).

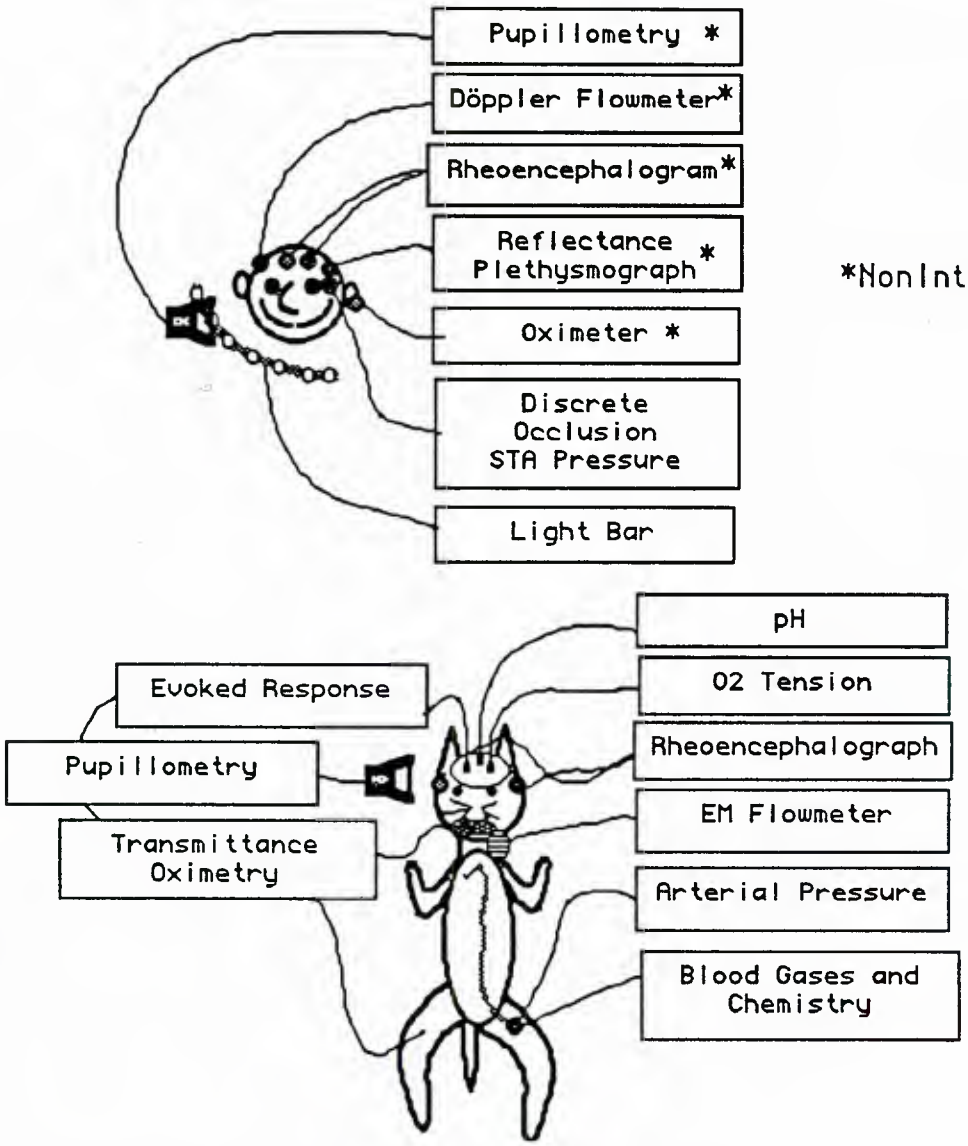

Figure 14. Components of a "Holistic" Approach to Monitoring

Committee for the Protection of Human Subjects (CPHS) Application

Non-invasive Evaluation of Cephalic Blood Flow in the +Gz Environment

Dr. Leon Hrebien, Barry S. Shender , M.S., and Dr. Stephen Dubin
(Contract No. N62269-85-C-0257,
Naval Air Development Center, Warminster, PA 18974.)

OBJECTIVES:

The purpose of this study is to construct and validate the use of a rheoencephalograph (REG) for evaluating the state of the circulation of the brain and sensory organs in a non-invasive and non-intrusive way. Another goal is the acquisition of knowledge leading to a better understanding of the pathophysiology of gravitational stress at the molecular level along with insights into means of mitigating or ameliorating this stress. The application for this study is for a period of three years, including annual reviews.

BACKGROUND:

The operation of modern combat aircraft may impose physiologic stress at or beyond the limits of normal toleration. In the case of gravitational force directed in the footward direction (+Gz), the effect may be loss of vision followed by loss of consciousness resulting from impaired circulation. These misadventures are particularly detrimental because they are rapid in onset, their occurance is somewhat unpredictable and they limit the most important sensory inputs of the crew-member. Such occurences place in jeopardy not only the health of the crew, but also the successful completion of a vital and sensitive mission. The ability to anticipate these events and to evaluate devices or maneuvers for protection is hindered by deficiencies in methodology and basic understanding. In particular, a major emphasis in dealing with the problem of peripheral light loss (PLL) and loss of consciousness (LOC) under +Gz, has been concern with maintenance of blood flow in the cerebral circulation. There is no doubt of the importance of such blood flow in the long term homeostasis of the central nervous system; however we speculate that, over the periods of interest in preventing PLL and LOC, consideration of cephalic blood volume may be of equal or greater importance.

Among tantalizing observations in the area of +Gz tolerance may be found the following: (a) Respiratory maneuvers found to be helpful in postponing PLL and LOC in the short run are of a general nature that is detrimental to circulation in the long run. (b) The onset of PLL and LOC (in common with syncope at 1G) seems rather sudden to be explained by loss of flow alone. (c) Net negative blood velocities, when measured by the Doppler ultrasonic method, have been observed in the superior temporal artery for extended periods of time under +Gz stress without significant decrease in pilot performance[1].

Insight into these observations is aided by consideration of some basic physiologic features of neural tissues. These tissues, including the retina and brain, have closely regulated but barely adequate blood circulation to supply nutrients (oxygen, glucose, etc) and remove waste - in contrast with organs such as skin, gut, and kidney whose abundant blood supplies reflect their circulatory interface function. Neural tissue comprises only three percent of body weight while receiving about 15% of the cardiac output and consuming about 25% of the oxygen. In the retina and in neural grey matter, oxygen consumption can be as high as 12 ml/100gm/min. By comparison with cardiac and skeletal muscles (having a similarly high oxygen extraction fraction), neural tissues lack an "on-board" oxygen buffer such as myoglobin. In the brain, oxygen is used only in the "terminal respiratory chain" of enzymes for oxidative phosphorylation in the mitochondria, i.e. ATP synthesis. This process is usually limited by the supply of ADP and inorganic phosphate rather than oxygen tension. Oxygen uptake by mitochondrial suspensions will continue until

the local partial pressure of oxygen falls to 0.1 mm hg.[2]. Therefore, when oxygen supply becomes limiting, it is because the volume or mass of oxygen has been exhausted.

The oxygen consumption in the brain is 40 - 50 ml/min. There is only 1.5 ml of oxygen dissolved in the tissue. The 75 ml of blood in the cerebral circulation contains about 15 ml of oxygen, mostly combined with hemoglobin. Therefore the hemoglobin in blood is the major oxygen buffer for the neural tissues. In our view, PLL and LOC under +Gz are caused not only by interruption of blood flow to the head, but also by removal of the major proportion of available oxygen. This view is consistant with observations of the retinal vessels under direct ophthalmoscopic observation using fluorescein as an indicator. During +Gz not only is there a total cessation of pulsatile flow but an apparent backward flow of fluoresecein dyed arterial blood from distal ophthalmic artery towards the carotid system. At offset of gravitational stress (G), the dye then returns to the ophthalmic artery and then is cleared from the arterial system [3]. Thus the benefits, during the short term, of G protective respiratory maneuvers may arise from "tidal" replacement and redistribution of the blood rather than actual net flow. To the extent that these speculations are applicable, three suggestions emerge: (a) The effects of +Gz on the oxygen availability to neural tissues as well as benefits of G protective maneuvers will be reflected in cephalic blood volume changes (plethysmography). (b) Mathematical modeling for simulation of G effects on PLL and LOC should account for distribution of oxygen supply as reflected in cephalic blood volume changes. (c) Studies relating to G tolerance and protection should consider other aspects of the oxygen buffering of neural tissue by blood including hemoglobin concentration, and the allosteric effects of such substances as 2DPG concentration, carbon monoxide, etc.

Several basic classes of measurement methods are currently being used or might be considered for use in the evaluation of the circulation in the +Gz environment.

1. Direct *in situ* measurement: Both electromagnetic and ultrasonic flowprobes are available for implantation on blood vessels such as the carotid artery. These are the "gold standard" for blood flow measurement. Their major disadvantage is, of course, the need for surgical implantation; absolutely precluding their use in humans. Another factor to be considered is the presence of multiple sources of cephalic blood flow (two each of the carotid and vertebral arteries along with the dorsal spinal artery).

2. Behavioral Methods: These rely upon a response or performance on the part of the subject. An example of such a method is the "NADC Light Bar." Although generally non-invasive, these methods are intrusive - they require the attention and participation of the subject; thus they are not suitable for in-flight use, nor are they readily applicable to animal studies.

3. Neurophysiologic Methods: The electroencephalogram, in its conventional form, is complex to intrepret. Alterations due to ischemic anoxia of the brain require four to fifteen seconds to appear. Visual evoked response testing shows potential application, but the equipment and data processing requirements are monumental.

4. Transcutaneous Ultrasonic Blood Velocity Methods: Among conventional methods used in "G" studies, application of transcutaneous ultrasonic blood velocity measurement to the external carotid and/or superior temporal arteries provide the most precisely quantitative estimate of the cephalic circulation. Stability of the probe placement is a significant problem. Other uncertainties relating to the use of ultrasonic blood velocity measurement under +Gz have been discussed at length [2].

5. Moderately Invasive Clinical Methods: These include indicator dilution methods for blood flow and contrast radiography (carotid arteriogram). Not only are these unacceptably dangerous to the subject, but also the flow information is an average over five to twenty heartbeats - hardly acceptable for events of such rapid onset as PLL.

In the late 1960's and early 1970's, the use of rheoencephalography (impedance plethysmography of the cephaliccirculation) held high promise in clinical neurology. The method is noninvasive, convenient, and adaptable to both patient monitoring and diagnosis of cerebral vascular disorders. It is non-intrusive and objective. Some problems attributed to rheoencephalography (REG) include a relative lack of anatomic selectivity and rather major signal "artifacts" upon changes in posture (particularly in the craniocaudal axis) and respiratory efforts, such as the Valsalva maneuver. We have

chosen to use the REG for the evaluation of cephalic circulation under conditions of gravitational stress because the very same "artifact" which apparently interferes with the use of REG in clinical neurology is of critical interest in G studies; namely, the bulk movement of blood between the head and the rest of the body with postural (gravitational) changes and respiratory maneuvers. Also, we are interested in studying total cephalic circulation not just the intracranial component. The basic design of the rheoencephalograph is, conceptually, very simple. The body segment to be examined is connected to a resistance bridge. The excitation source of the bridge is generally sinusoidal in the frequency range of 15 to 150 kHz. Currents in this frequency range will not effectively stimulate the heart or skeletal muscle. The output of the bridge is amplified and demodulated. A major challenge in recording the REG is the composite nature of the impedance changes that are recorded. The resting baseline impedance is determined by the composition (blood, bone, etc) of the body part being examined, its geometry, and the electrode interface. Bulk shifts of blood, such as result from venous occlusion of a limb, the Valsalva maneuver or G forces cause changes in the range of 1-2% of the total baseline value. Resistance changes resulting from arterial pulsations are three orders of magnitude smaller than the baseline resistance. With previous circuits and display devices, acquisition of the pulsatile component resulted in loss of much information about the bulk blood shifts.

Much of our initial work has been devoted to application of more recent improvements in electronic instrumentation, including digital methods, to the acquisition of the REG. In our design efforts, real time signal processing has been a priority. Among the technical problems we have addressed are: a). separation of baseline impedance (Zb) from change in impedance due to pulsatile variation in blood volume (ΔZ), b). amplification of ΔZ, c). noise reduction, d). shock hazard reduction, e). electrode configuration, f). G "hardness."

Preliminary evaluation of our REG instrument has shown the following [4]:

1. The instrument has been installed on the NADC centrifuge and subjected to 10 g without decrement in its performance.

2. In animal and human experiments "on the ground" the instrument has performed well. In particular, the ability to separate the faster (pulsatile) components of the REG from the slower changes referable to bulk movement of blood between the head and the rest of the body, have permitted the study of the pulsatile component in much greater detail. Respiratory manuveurs not only induce a shift in the baseline, but also introduce significant changes in the pattern of the pulsatile component itself. We believe this devolves from the interplay of blood circulation with shifts of cerebrospinal fluid.

3. When used in the centrifuge gondola on a subject not subjected to gravitational stress, the instrument was able to produce reliable recordings even when the output signal was passed through the slip-ring system twice. A sample of such a recording is shown below.

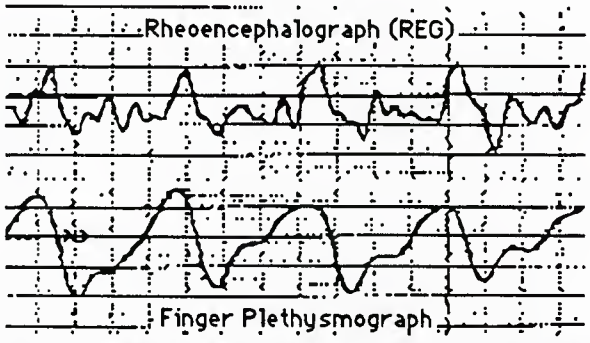

Recording of Rheoencephalograph and Finger Plethysmograph
Made in Human Centrifuge Gondola (No G Stress)

ABSTRACT:

Impairment of vision and consciousness under gravitational stress in the footward direction (+Gz) has been attributed primarily to interruption of blod flow to the brain and retina. During the initial phase of +Gz, the volume of blood available to neural tissues is also a significant factor because of the oxygen buffering function of hemoglobin. The rheoencephalogram (REG) reflects changes in cephalic blood volume and is convenient, non-invasive and non-intrusive. As part of our preliminary work, some of the drawbacks previously perceived for the REG have been ameliorated through technical innovation; while others have been proven not to be of concern. Indeed, the "artifact" seen with position changes and respiratory maneuvers is actually a source of useful information in the context of +Gz studies. The current phase of investigation for which approval is requested involves the application of the REG during centrifuge flights otherwise scheduled and authorised for physiologic investigations. The addition of the REG will neither impair the scheduled studies nor will it add any risk. Indeed, the REG will permit another mode of monitoring the cephalic circulation and thus promote the safety of the subjects.

PROTOCOL:

Please note that in this section and in subsequent ones, discussion is limited to the use and investigation of the rheoencephalograph instrument. The studies will be performed in connection with other approved experimentation for the study of physiologic response to and protection for gravitational stress.

Detailed instructions for the operation of the REG instrument are appended. Briefly, the skin of the forehead of the subject is cleansed with soap and the skin is lightly abbraded with a paper towel. The skin is then cleaned with alcohol to remove oils. The electrodes are cleaned with alcohol and a small amount of conductive gel is applied. The electrodes are initially applied to the forehead with small pieces of hypoallergenic tape. An athletic headband is the used to cover the electrode montage and promote adherence. After the electrode cable is connected to the REG instrument, adjustments are made and the output signals are transmitted through the slip - ring system to the "flight deck" and recording instruments. The signals to be recorded are the pulsatile and "slow" portions of the REG.

Data for study will consist of the REG signals along with other physical (G profile) and physiologic (EKG, Doppler flowmeter, Visual field, etc) data which are concurrently acquired. Analysis of the data will be performed in order to evaluate the following:

1. What is the quality of performance of the instrument under the physical conditions of the experiments?
2. What interractions occur between physiologic alterations (heart rate changes, etc) that occur under G stress and the performance of the REG instrument?
3. What interractions occur between protective maneuvers and/or devices and the performance of the REG instrument?
4. What changes occur in the REG signals which may be related to physiologic response to the +Gz stress and/or protective maneuvers or devices?
5. What is the temporal relationship of changes seen in the REG signal to any episodes of peripheral vision impairment or loss of consciousness that may occur during the experiment ?

BENEFITS:

The primary immediate benefit of this phase of investigation is the validation of a method for immediate continuous evaluation of the circulation of the brain and special sensory organs (REG) under conditions that are controlled and reproducable while still realistically simulating those existing during the operation of high performance aircraft. The method is safe, convenient and non-invasive. It is also objective and non-intrusive; it does not require the attention of the subject or interfere with mission tasks. It is our viewpoint - a matter to be settled in part by this series of experiments - that the REG will provide a superior means of anticipating the occurence of PLL and LOC under G stress and to evaluate devices or maneuvers for protection against these misadventures. In this way it may well improve the safety of the current experiments for the subjects.

A less immediate but nontheless significant potentiual benefit is derived from the ability of these studies to reveal new information both about the interraction of +Gz stress with the sensory integrity of crewpersons and about the general "economy" of the nervous system with respect to supply and utilization of oxygen.

RISKS:

Because the rheoencephalograph, in common with many common clinical instruments, makes electrical contact with the skin of the subject; it is necessary to consider the potential risk related to electrical currents. In estimating such risks, one should consider the following: a. the magnitude of currents that may flow, b. the location of the electrodes and c. the frequency of the current that may be passed. Our REG instrument is operated by internal battery power with no connection to the power lines or other source of electricity. The maximum voltage existing anywhere in the instrument is ±9 v. The bridge circuit is connected to electrodes placed on the forehead or nasal bridge of the subject. The current used for operation of the bridge circuit is at a frequency of 100 kHz and is limited to values of less than six microamperes. For purposes of comparison it should be noted that the situation of greatest vulnerability to electrical risk occurs when a current is applied to the myocardium possibly leading to ventricular fibrillation. Ventricular fibrillation is most likely with stimulation frequencies at close to that of house current (50 - 60 Hz.). At such frequencies, a current of 100 microamperes need be applied to the myocardium or 100 milliamperes need be applied to the skin over the heart in order to induce ventricular fibrillation. For this reason the maximum leakage current for power lines operated instruments (such as electrocardiograph machines) which may pass 60 Hz. current to the myocardium is limited to ten microamperes. At high frequencies such as that produced by our REG instrument, the current necessary for ventricular fibrillation is much higher; indeed it may not be possible to induce ventricular fibrillation with 100 kHz. currents. For currents at 100kHz. applied to the skin, other possible adverse effects might be involuntary skeletal muscle contraction for which a current of 16 milliamperes is needed; and local burning for which a current of above one ampere is required. To summarize the predictable risks related to electrical current, our REG device utilizes a current which is of a frequency, magnitude and site of application that reasonably precludes any of the known electrical risks [5].

An additional risk associated with the skin electrodes is local allergic response. The existence of this risk is inferred from the moderately frequent observation of contact dermatitis related to use of jewelry. When present, this is usually seen as a local hyperemia and irritation. Although possibly uncomfortable, this condition is transient and reversable with removel of the inciting allergen. We pay particular attention to this risk, however, because the existence of blemishes on the forehead is cosmetically undesirable. The electrodes for our study are those conventionally used for application to the forehead and scalp in electroencephalograph and biofeedback studies. They are made of gold, silver or nickel ("German silver") alloy. In our study we intend to further minimise this risk by asking subjects whether they have ever had any reaction to any metals or jewelry and to report immediately any persistant irritation or mark at the electrode site(s) that could not be attributed to the physical presence of the electrode alone.

SUBJECT POOL:

The subjects will be physically qualified volunteers otherwise suitable for acceleration studies except that individuals having a history or recollection of allergy or sensitivity to gold, silver, nickel or other metal or jewelry will be excluded from the REG portion of the study.

BIBLIOGRAPHY:

1. Johanson, D.C. "An Investigation of the Apparent Negative Velocities of Cerebral Blood Flow During Exposure to +Gz Acceleration." Thesis, Drexel University, Philadelphia PA, 1982.

2. Honig, C.R.: Modern Cardiovascular Physiology. Little Brown & Co, Boston, 1981.

3. Leverett, S.D.: Aerospace Physiology and Medicine in Medical Engineering. (C.D. Ray editor) Chicago, Year Book Medical Publishers 1974 (p 827).

4. Shender, B., Dubin, S., Hrebien, L., Barnea, O. and Kepics, F.: "Rheoencephalography: The Jury is Still Out." Proc. 13th Bioeng. Conf. In Press.

5. Directions in Cardiovascular Medicine 3: Book IX. The Heart and Electrical Hazards. Hoechst Pharmaceuticals, Somerville NJ 1983.

INSTRUCTIONS FOR USE OF THE RHEOENCEPHALOGRAPH (REG)

1. ELECTRODE SITE SELECTION: The REG will provide an overall view of the cephalic circulation rather than provide specific information about localized blood volume changes. However, a bioccipital placement will preferentially show vertebral artery circulation and bitemporal placement will favor carotid artery volume changes. In either case, choose an area of the skull in which movement artifact will be minimized, i.e. not over the mandibles or directly next to the ectocanthus (picks up eyeblinks).

2. SKIN PREPARATION: The area under the electrodes must first be cleansed with soap and abraided lightly (e.g. with paper towel). Next apply alcohol to remove any remaining oils.

3. ELECTRODE APPLICATION: There are two electrodes attached to the skull. If one uses the Sentry Medical Sentry Silver Sircuit Pediatric® electrodes, remove two from the package, add a few drops of water the activate the adhesive and place on the skin. Electrodes may be repositioned (add more water if necessary) and are designed to last at least 15 days. Complete instructions are found on the reverse of the package. If one choses to use the stainless steel disk electrodes, apply electrode paste to the electrodes and attach them to the head using surgical or first aid tape.

3a. Insert the electrodes into banana jacks provided in the front of the REG or in the extension cable. Place the plugs into the outer two jacks. The center jack should be left disconnected.

4. BALANCING THE BRIDGE CIRCUIT: Attach two BNC cables to the connectors marked **HEAD O/P** to the inputs of a differential amplifier. This amplifier is then connected to an oscilloscope to monitor the AM modulated output. Using the bridge **COARSE ADJUST** potentiometer, adjust the output sinusoidal waveform until it reaches a value between 50 - 100 mV peak-peak. Observe the pulsatile REG waveform (Zp) output from the BNC terminal marked **PUL. Z.** If the signal is too noisy, then use the bridge **FINE ADJUST** potentiometer until the waveform is satisfactory. Since the bridge works "off-null" many different subjects may be monitored without much bridge adjustment if one prepares the electrode sites properly.

5. Zp GAIN: Additional gain (26-75 times) can be applied to the Zp waveform by using the **Zp GAIN** potentiometer. The output Zp waveform can be inverted if necessary by switching the **INVERT** switch to the opposite position.

6. BASELINE IMPEDANCE: To monitor the baseline impedance (Zb) attach a BNC cable to an oscilloscope or recording device to the jack marked **BASE Z**. Correction for dc offset in Zb, if necessary, is possible via the **Zb OFFSET** potentiometer. Additional gain is possible via the **Zb GAIN** potentiometer.

7. HEAD RESISTANCE AND CALIBRATION: One can measure the overall resistance of the

head by connecting the **Ro** BNC jack to a dc voltage meter. The voltage can be converted to ohms by switching the **CAL** switch from **NOP** to the right. This produces a 1Ω change in the output with which to convert the dc voltage to ohms. Similarly, one can use the **CAL** switch to calibrate the Zp and Zb voltage waveforms to ohms.

8. POWER SWITCHES: The REG has two battery power supplies. Two 9 volt alkaline batteries supply the oscillator and are accessed through the back panel. The ON/OFF switch is also mounted on the back panel. The rest of the circuitry is powered by 12 "C" cell alkaline batteries found in two battery holders in the bottom of the circuit card cage. The replace these batteries, remove these holders from the battery connectors found under the circuit boards directly behind the mother board. Carefully replace these holders observing the correct polarity of the connectors. The ON/OFF switch is mounted on the front panel.

9. TROUBLESHOOTING:

a). If a clear output waveform cannot be obtained check the following:

i). Check the electrode contacts on the head for secure fit and enough electrode gel (be careful not to apply too much gel or it will leak out onto the securing tape and loosen the electrodes).

ii). The signal may either be saturated or set too low for the demodulator to function. Check the signal at the jacks marked **BP1 O/P** and **BP2 O/P** for saturation or a signal < 0.7 V peak-to-peak. There are adjustment pots at the beginning of each stage. Use the 20kΩ pot of BP1 first to adjust the gain then, if necessary, use the 50 kΩ pot of BP2. Check the output at the jack marked **LPF O/P** for proper gain setting (a rectified output of 2-4 volts is sufficent).

b). To check the output of the instrumentation amplifier connect a BNC cable from the **BP I/P** jack to an oscilloscope.

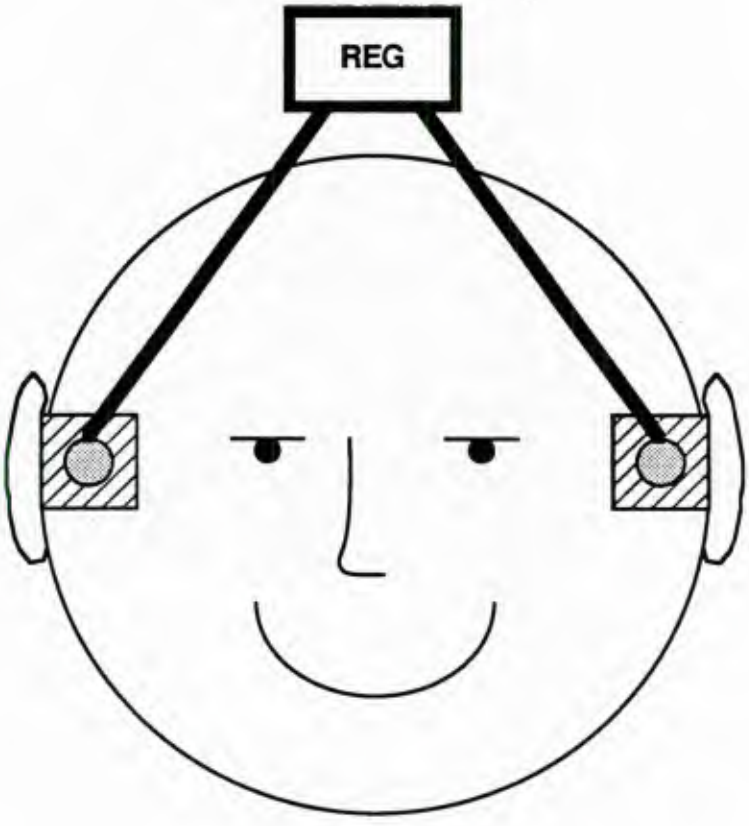

KEY for REG Electrode Placement

(NOTE: Electrodes are placed Bitemporally)

Electrode Cable To REG

Signal Electrode

Adhesive Tape To Secure Stainless Steel Electrodes

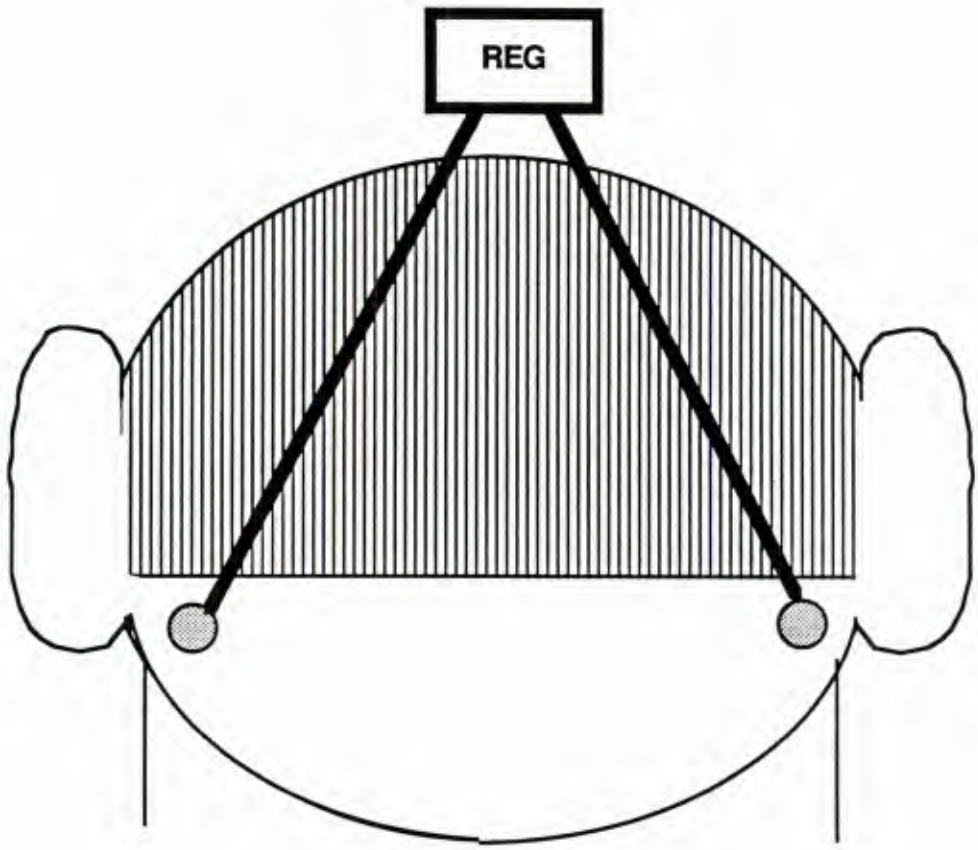

KEY for REG Electrode Placement

(NOTE: Electrodes are placed Bioccipitally)

Electrode Cable To REG

Signal Electrode

(NOTE:
Sentry Medical Electrodes do not require adhesive tape)

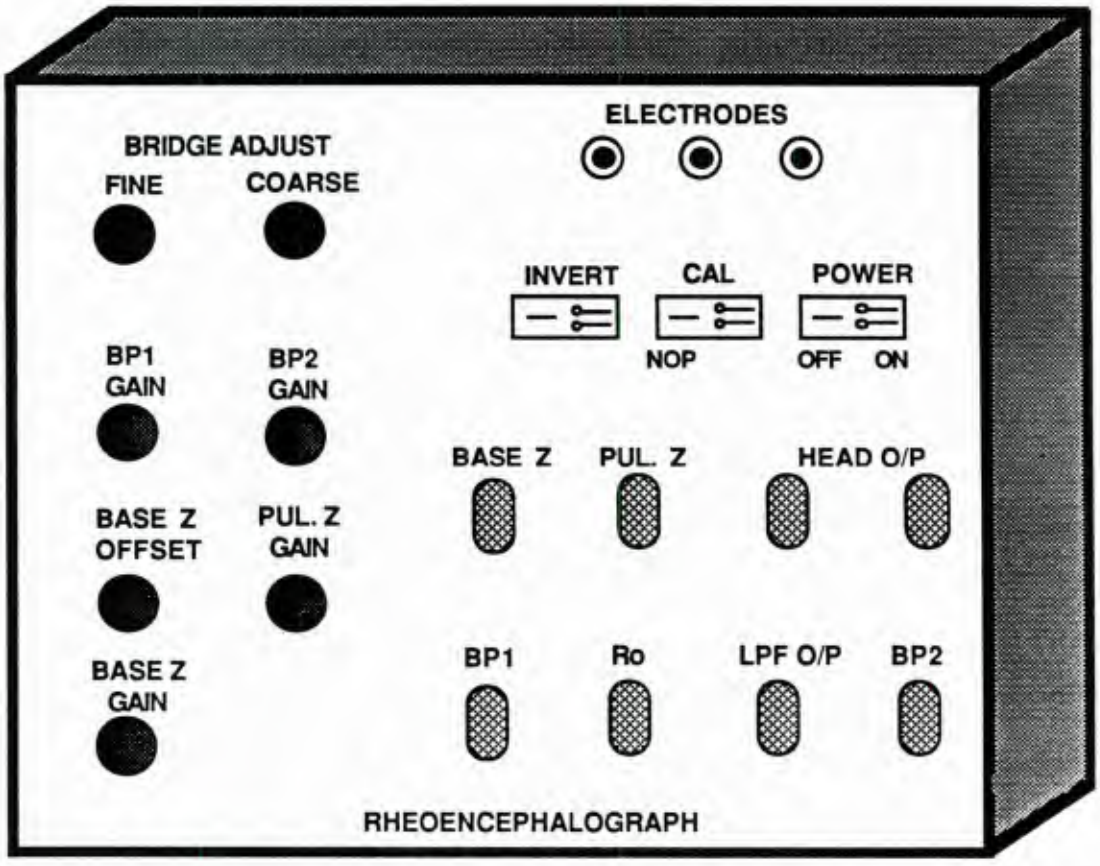

KEY FOR RHEOENCEPHALOGRAPH

- Adjustment Knob
- BNC Socket
- Electrode Pin Socket
- Switch

DISTRIBUTION LIST

	No. of Copies
Direct, Defense Technical Information Center	12
Commander, Naval Air Systems Command	6
(3 for AIR-320R)	
(2 for AIR-931H)	
(1 for AIR-531B)	
Office of Naval Technology	2
(1 for ONT-223)	
Commanding Officer, Naval Medical Research & Development Command	2
(1 for NMRDC-44)	
Chief, Bureau of Medical & Surgery	2
(1 for NM&S 3C1)	
Chief of Naval Operations	3
(1 for NOP-05H)	
(1 for NOP-09E)	
Chief of Naval Research	5
(1 for ONR-440)	
(1 for ONR-441)	
(1 for ONR-441NP)	
(1 for ONR-442)	
Commander, Naval Safety Center	1
Commanding Officer, Naval Aerospace Medical Research Laboratory	1
Superintendent, Naval Postgraduate School	1
Commanding Officer, Naval Health Research Center	1
Commanding Officer, Naval Personnel Research & Development Center	1
Commander, Naval Air Test Center	1
Commanding Officer, Naval Biodynamics Laboratory	1
Commanding Officer, Naval Submarine Medical Research Laboratory	1
Commanding Officer, Naval Training Equipment Center	1
Air Force Office of Scientific Research (AFSC)/NL	1
Air Force Aerospace Medical Research Laboratory	2
U.S. Air Force School of Aerospace Medicine	1
U.S. Army Aeromedical Research Laboratory	1
FAA Civil Aeromedical Institute	1
NASA Ames Research Center	2
NASA Johnson Space Center	1
Dr. Banu Onaral, Drexel University	2
Dr. Dov Jaron, Director Biomedical Engineering & Science Institute, Drexel University	1
Center for Naval Analyses	1